Optimization of the Electrical Anisotropy of Composite Molybdenum Disulphide Films

by

Hong Tang

B.Sc., Jilin University, 1984

THESIS SUBMITTED IN PARTIAL FULFILLMENT OF
THE REQUIREMENT FOR THE DEGREE OF
Master of Science

in the department

of

Physics

Simon Fraser University

December 1991

Approval

Name: Hong Tang

Degree: Master of Science

Title of Thesis: Optimization of the Electrical Anisotropy of Composite MoS_2 Films

Examining Committee:

Chair: Dr. E.D. Crozier

Dr. S.R. Morrison
Senior Supervisor
Professor
Department of Physics

Dr. R.F. Frindt
Professor
Department of Physics

Dr. A.E. Curzon
Professor
Department of Physics

Dr. K. Colbow
External Examiner
Professor
Department of Physics

Date Approved December 2, 1991

PARTIAL COPYRIGHT LICENSE

I hereby grant to Simon Fraser University the right to lend my thesis, project or extended essay (the title of which is shown below) to users of the Simon Fraser University Library, and to make partial or single copies only for such users or in response to a request from the library of any other university, or other educational institution, on its own behalf or for one of its users. I further agree that permission for multiple copying of this work for scholarly purposes may be granted by me or the Dean of Graduate Studies. It is understood that copying or publication of this work for financial gain shall not be allowed without my written permission.

Title of Thesis/Project/Extended Essay

OPTIMIZATION OF THE ELECTRICAL ANISOTROPY OF COMPOSITE MoS_2 FILMS

Author: _____
(Signature)

HONG TANG
(Name)

Oct. 24, 1991
(Date)

ABSTRACT

Molybdenum disulphide(MoS_2) has been exfoliated into monolayers by intercalation with lithium (Li) followed by reaction with water. X-ray diffraction analysis has shown that the exfoliated MoS_2 in suspension is in the form of one-molecule-thick sheets.

Single molecular layers of MoS_2 (and other layered materials as well) prepared in the form of a suspension in water can be collected at a water-organic solvent (water immiscible) interface, a location energetically preferred by the layers. Furthermore, due to the so-called Marangoni effects, spontaneous spreading from the interface can be employed to prepare large area, optical quality, highly oriented films several hundred angstroms thick on various kinds of substrates.

The exfoliated MoS_2 platelets are surrounded by OH^- groups when in suspension, which enables us to modify the single layer configuration by attaching or substituting different kinds of desired species onto the basal or edge planes of the platelets.

Using the spreading and modification techniques, we can obtain novel film materials which have interesting

characteristics and which include, for example, organic molecules such as polystyrene. The polystyrene appears between the layers in the van der Waals gaps whilst the oriented MoS_2 layers form a host lattice. Species such as metallic ions can be deposited, presumably on the edge planes, horizontally connecting neighboring platelets. Such molecular sandwiches may display high electrical anisotropy between directions parallel and perpendicular to the basal planes of the layers.

The objectives of the work were to study methods of varying the resistivities of the film in the above two directions and, by studying such methods, determine the conduction mechanism in the film. We examined metal ions deposited at the edges of the platelets, and were able to decrease the resistivity in the direction parallel to the layer basal planes by a factor of 10 (compared to an additive free film). We examined polystyrene included film and were able to increase the resistivity in the direction perpendicular to the layer basal planes by a factor of 10^3. The electrical anisotropy achieved in this work is around 10^6. Models to explain these results and the measurements are presented.

From such resistivity measurements, it is concluded that conductivity in the direction perpendicular to the layer

basal planes is dominated by direct electron hopping across the van der Waals gap, with an activation energy of 0.18eV. From measurements with Cu, Ni or Co ions present, it is concluded that the metal ions are only adsorbed at the edges of the platelets and their presence induces rings of high conductivity around the platelets and facilitates electron transfer from one platelet to another in a direction parallel to the basal planes of the layers.

The techniques and the composite films may have extended applications.

DEDICATION

TO MY WIFE Li Lan

ACKNOWLEDGEMENT

I wish to express my deepest gratitude to Prof. S Roy Morrison, my senior supervisor, for sparing his valuable time to guide me in carrying out this study and for his encouragement and support. Profs. R.F. Frindt and A.E. Curzon , members of my supervisory committee, are thanked for their concerns over the thesis project progress. I would also wish to thank Drs. W.M.R. Divigalpitiya and B. Miredadi for their hands on help and their kindness.

TABLE OF CONTENTS

LIST OF TABLES

$*\rho_{//}$ film resistivity in the direction parallel to the basal planes of the layers

$**\rho_{\perp}$ film resistivity in the direction perpendicular to the basal planes of the layers

LIST OF FIGURES

*$\sigma_{//}$ conductivity in the direction parallel to the platelet basal planes

**$\sigma_{\perp}$ conductivity in the direction perpendicular to the platelet basal planes

CHAPTER I INTRODUCTION

1.1 GENERAL INFORMATION ON TRANSITION METAL DICHALCOGENIDES (TMD) COMPOUNDS

1.1.1 Transition metal dichalcogenides

The transition metal dichalcogenides (TMDs) are about 60 in number and two-thirds of them assume a layered structure [1]. The layered compounds are often considered to be two dimensional because of high anisotropy resulting from strong bonding within the layers and weak inter-layer interactions. For some time there has been a wide interest in two dimensional systems from both theoretical and experimental points of view. Additional interest arises from the fact that they can be intercalated with a variety of metals and compounds. Several special topics concerning various aspects of the properties of these materials have been of particular interest, such as exciton screening; d-band formation and metal/insulator transitions; also magnetism and superconductivity in such compounds [1]. In this thesis project, MoS_2 (an important member of the TMD family) was studied. The main object was to study the electrical anisotropy of polycrystalline MoS_2 films, using some particular techniques (to be described) to influence the resistivities.

1.1.2 Structures of TMDs

The structures of the TX2 dichalcogenides(T: Transition metal; X: chalcogenide) fall into two distinct classes, namely, layered and otherwise. The layered materials arise from the stacking of hexagonally packed planes (not close packed). The coordination around the metal atoms is either trigonal prismatic (e.g. MoS_2, NbS_2) or octahedral (e.g. HfS_2, PtS_2). The coordination around the non-metal is quite lopsided, and this leads to the marked ease of cleavage perpendicular to the hexagonal/trigonal symmetry axis (c). The basic atomic structure of the loosely coupled X-T-X atom sheet sandwiches makes such materials extremely anisotropic both mechanically and electrically. The molecular sheets are loosely bounded together by van der Waals force (v.d.W.bonding) and the gaps between the sheets are called van der Waals gaps.

1.1.3 Properties of layered TMDs

The extremely anisotropic character of the layered compounds, built in at the atomic level, dominates all the properties of such materials, both mechanical and electrical. The expansion coefficient is about a factor of 10 greater perpendicular to the layers than parallel [2], conversely the velocity of sound in the parallel direction is twice that perpendicular to the layers [3]. The thermal conductivity is also higher by almost a factor of 10 parallel to the layers

[3]. Under applied pressure this anisotropy falls rapidly as the structure stiffens mechanically [3]. Electrical conduction is even more anisotropic, at least for MoS_2 where a difference factor of 10^3 has been reported [4]. This is the subject to be discussed in detail in this thesis.

Another result of the weak van der Waals bonding is that the inter-sandwich gap will open up to accept alkali metal ions from ammonia solution and other sources [1]. This process is named intercalation.

1.2 MOLYBDENUM DISULPHIDE, MoS_2

The properties of molybdenum disulphide have been widely studied in the past. An appreciable amount of information has been accumulated. The present study concentrates on the electrical conducting properties of this material in new configurations unavailable before.

1.2.1 Structural anisotropy

MoS_2 is the only member, in the layered TMD family, that occurs naturally in appreciable quantity. Naturally occurring MoS_2 has been found in the 3R as well as the common 2H sandwich stacking [5]. The two types belong to different space groups. The 2H-MoS_2 is remarkably stable to pressure, temperature (up to 1000°C) and crystal composition [1]. A single layer of MoS_2 consists of a sheet of Mo atoms

sandwiched between two sheets of S atoms. In 2H-MoS_2, there are two layers per unit cell. The van der Waals gap between the two layers is 2.96Å and the distance between the two S atom sheets within a single layer is 3.19Å while the distance between Mo atoms on adjacent sheets is 6.41Å. In addition, within a single layer, the S atoms are 2.41Å away from their neighboring Mo atoms (Fig.1). The density of the 2H-MoS_2 is 4.92×10^3 kg/m^3 [6] and the density of 3R-MoS_2 is 5.00×10^3 kg/m^3 [7]. The weak inter-layer bonding leads to the observed MoS_2 cleavage properties.

1.2.2 Band structure

Fig.2 illustrates the general types of inter-band transition for the trigonal prism group VI compounds (which include 2H-MoS_2). The values correspond to those calculated for MoS_2. The degree of filling of the d bands lying between the basic bonding-antibonding gap (about 4ev in MoS_2), in principle, determines the electrical character of the various compounds. Several factors affect the form of the d band.

(a) inter-layer distance, T-X, T-T and X-X (size factor)

(b) ligand electronegativity (energy factor)

(c) detailed electronic configuration of metal atom

(d) crystal structure (symmetry factor)

These factors are of course inter-related [1].

A significant degree of d and p covalent mixing into the valence band along with the metal s states seems feasible in

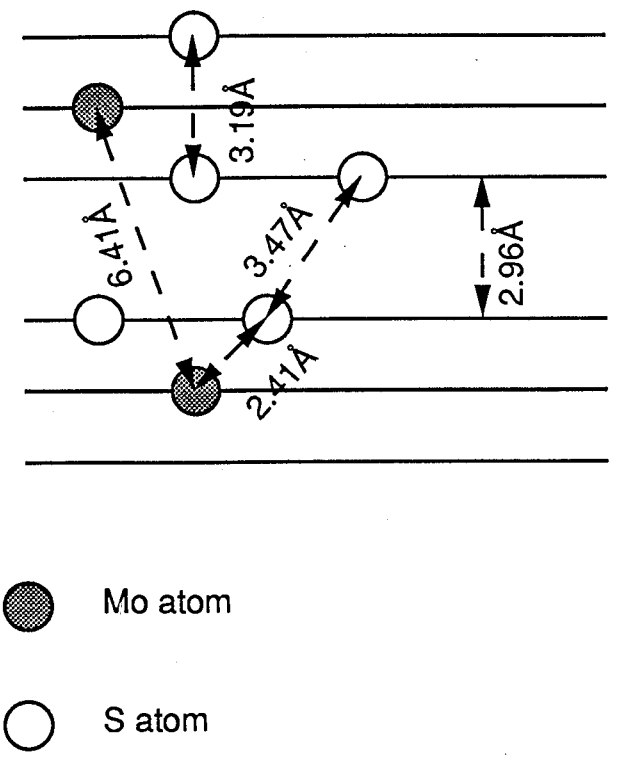

Fig.1 Layered structure of MoS_2

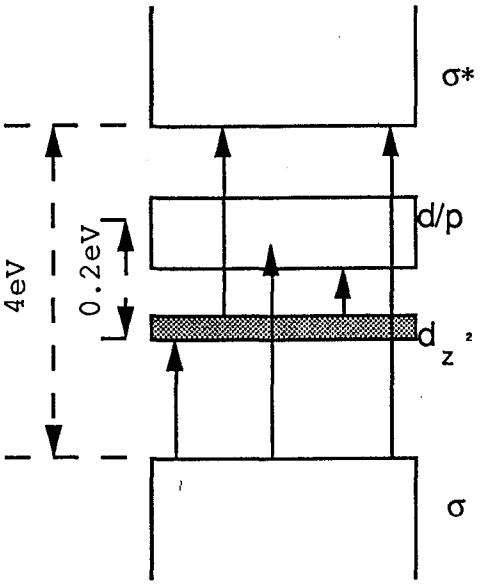

Fig.2 General types of interband optical transitions

the dichalcogenides. When the distance between metal atoms (in a layer) increases, as in a compound, this direct metal sublattice mixing decreases rapidly, particularly to the center right of each series where the atomic radii are small. The metal-metal distance in a layer of MoS_2 is 3.16Å which corresponds to 15% increase over that in the pure metal. With covalent bonding, the valence band is considerably broader due to T/X state mixing. In a transition metal compound like MoS_2, it is likely that the mixing of metal states into the valence band follows the pattern s > d >>p. The p states are more likely to be mixed into the energetically closer non-bonding d bands, interposed within the basic $\sigma\sigma^*$ gap.

In a structure with trigonal prism coordination as in MoS_2, the d states split in such a way that the d_{yz} and d_{xz} orbitals are the most likely to mix into the valence band. The $d_{x^2-y^2}$ and d_{xy} orbitals will mix more with the metal p_x and p_y states, and are likely to form a non-bonding band above and detached from a second non-bonding band based on d_{z^2}. This latter orbital gives poor overlap between near-neighbour metal atoms and the band is likely to be rather narrow. The transition across the d band (from d_{z^2} to d/p, 0.2ev for MoS_2 at the IR edge) is now known to determine the whole character of the electrical properties of the group VI semiconductor (MoS_2) family [1,8](Fig.2). However, the electrical properties

of the MoS_2 films we made seem little connection to the band model in Fig.2.

1.2.3 Electrical anisotropy

The structural anisotropy of MoS_2 (also other layered compounds) results in significant electrical anisotropy. The electrical conductivity in the layer plane is much higher than that across the layers. For MoS_2, the conductivities may differ in these two characteristic directions by a factor of 10^3. A number of workers had previously made electrical measurements on MoS_2 crystal [9 - 17] with fairly scattered results because the electrical measurements on single crystals of MoS_2 have proved very difficult, due to the layered character of this material. The crystal edges are exceedingly soft and any damage on a microscopic level must lead to extensive "elimination" of the high electrical anisotropy of the sandwiches [1]. In addition it has been claimed that good contacts for such measurement are also difficult to make [14,18]. Because of these factors, the results collected to date differ from each other dramatically, e.g. measured resistivity perpendicular to the layers varies from 10^3 to 10^5 Ω.cm while the measured resistivity parallel to the layers varies from 10 to 10^3 Ω.cm. These measurements were made on single crystals (most of them naturally occurring, from different geological locations which could be partially responsible for the

scattered results). The samples used in this thesis project are polycrystalline and the electrical properties of the boundaries are expected to dominate [18]. Preliminary work on resistivities of blank samples (pure MoS_2 without additives) of this type has been already done and resistivities of approximately 10^4 Ω.cm parallel to the layers and 10^6 Ω.cm across for blank films were reported [19].

1.3 GROWTH OF MoS_2 CRYSTALS

A number of methods to obtain MoS_2 crystals have been reported. A unique feature of the technique used in this study is that it produces crystals which are polycrystalline, but with the layers highly oriented as in a single crystal.

1.3.1 Natural crystals

Natural crystals occur as a series of single crystal sections which are grown together with different orientations. They vary in size from chips only a few millimeters across to large multicrystal blocks which are over three centimeters on a side. The usual technique used to prepare single MoS_2 crystals from such a natural crystal is to cleave using cellotape. The thickness of samples so prepared can be as small as 500Å [1].

1.3.2 Synthetic crystals

MoS_2 crystals can be synthesized by different means. For instance, by heating the mixture of S(99.999) and Mo(99.99) in vacuum (10^{-6} torr.) at 700°C and in the appropriate temperature gradient [20,21], large 2H-MoS_2 crystal can be grown along the silica ampoule. Also, crystal can be grown by means of bromine transport [22] but the products were found to be in the rhombohedral (3R) polytype [23]. Bromine is not the only gas suitable for such a transport method [22].

1.3.3 Spreading polycrystals

Spread films were obtained by using the unique exfoliation and film fabrication techniques developed in our laboratory. The most significant difference between our samples and those used by other workers mentioned above is that our films are obviously polycrystalline and therefore the electrical properties of the boundaries are expected, to some extent, to mask the properties of the bulk single crystal. However, because the basal planes are highly oriented, the electrical anisotropy can still be observed. With some modifications, we have been able to enhance this anisotropy and because of this, such films may have potential interest and applications in various areas. The preparation of the spread films will be described in detail later.

1.4 MARANGONI EFFECTS

With the name of the Italian physicist Carlo Marangoni of Pavia and Florence (1840-1925) have been associated two distinct though related surface effects. The first of these is movement in a fluid interface. The motion is caused by local variations of surface tension that are caused in turn by differences in composition or temperature. The second is the conjugate of the first, it is the departure from equilibrium tension that is produced by extension or contraction of an interface [24]. Both effects were correctly explained in a qualitative way more than one hundred years ago. These effects are considered to be the basis for preparing the polycrystalline MoS_2 films [19].

1.5 OBJECTIVES OF THE PRESENT STUDY

This work has been aimed to study variations in composite films preparation, with the objective in part to make films with high electrical anisotropy and in part to pursue a better understanding of the electrical behavior of such films. The basic configuration of our films has a MoS_2 host lattice with the single layers of MoS_2 highly oriented parallel to the substrate. During the fabrication, various modifications using foreign additives were attempted and examined. They were designed to affect the electrical anisotropy originally possessed by MoS_2 films. Specifically the inclusion of most foreign species in the MoS_2 films is

only possible with the exfoliation and spreading techniques employed, and this clearly demonstrates the advantages of such techniques. We have been able to achieve an anisotropy in resistivities along and across the films by a factor of 10^6 and even higher.

CHAPTER II EXPERIMENTAL BACKGROUND

In this chapter, we summarize experimental techniques developed in our laboratory for the preparation of exfoliated MoS_2 and for the re-stacking of the MoS_2 in various forms.

2.1 PREPARATION OF SINGLE MoS_2 LAYERS

The method used to obtain single MoS_2 layers has been developed by other workers [26] in our group and consists of two basic steps, namely, Li intercalation and the actual exfoliation (separation of originally bonded single layers) that follows.

It is a well established phenomenon that the lamellar transition metal dichalcogenides as a class can serve as hosts for the intercalation of a variety of electron donating species [25]. Alkali-metal intercalates are essentially of ionic character as a consequence of the high electron affinity of the hosts

$$nA + TX_2 \rightarrow (A^+)_n TX_2^{n-}$$

where A is the alkali atom. The transfer of an electron to the host is corroborated by thermodynamic activity measurements, by lattice parameter expansions, and by the solid-state Nuclear Magnetic Resonance (NMR) chemical shifts

observed for the lithium case [25]. The starting material is 2H-MoS_2 powder (-325 mesh, 98%) from Materials Research Corporation. The MoS_2 was first soaked in a 2.5M solution of N-butyllithium in hexane for at least 48 h (in fact, we usually allow one week or longer for the intercalation), in a dry box containing an argon atmosphere. This intercalates the MoS_2 with lithium (Li_xMoS_2) to a mole fraction of at least $x = 1$ [26].

Following the intercalation of MoS_2 by lithium, the MoS_2 was removed, washed repeatedly (twice at least) in hexane, dried, and sealed in a vial, still in the dry box under argon atmosphere. The vial was then removed from the dry box, immersed in water and the cap removed from the vial. Upon contact with the water, copious gas evolution followed and the MoS_2 powder formed a highly opaque suspension in the water. It is assumed that the reaction between the water and the intercalated lithium forms hydrogen gas between the layers (in the van der Waals gaps).

$$Li + H_2O \rightarrow LiOH + 1/2H_2\uparrow$$

The expansion of the gas tends to separate (exfoliate) the layers. As the reaction proceeds more deeply into each crystalline grain the layers become further separated. Eventually the layers become completely separated and remain

suspended in the aqueous solution. The suspension was ultrasonicated during the reaction to assist in this reaction. The pH of the solution was moderately basic at this stage due to the presence of lithium hydroxide [26], which can be removed by repeated washing and centrifuging with distilled water, though the removal of Li^+ cannot be expected to be perfectly complete.

We shall frequently refer to the individual single layers of MoS_2, prepared in this way, as "platelets" at appropriate places in the rest of the thesis. It has been concluded [19] that the platelets stay in suspension because of the repulsion among the surface double layers associated with adsorbed OH^- groups.

2.2 RE-STACKING OF EXFOLIATED MoS_2

There are several ways to re-stack exfoliated MoS_2 platelets. However, different methods may result in different configurations, which may in turn satisfy various needs.

The MoS_2 platelets can be flocculated by lowering the pH. The exfoliated MoS_2 platelets can stay in suspension for a very long period of time (weeks or even months) at an intermediate pH, from say pH=3 to pH=10, while on the other hand the as-received unexfoliated MoS_2 suspension will settle down in minutes. One way to clear the suspension of

exfoliated MoS_2 is to cause flocculation by adding cations such as H^+ (in HNO_3 for instance) to reduce the suspension pH to pH<3. One example of taking advantage of the flocculating phenomenon is to make a house of cards house of cards (HOC) structure by flocculating the suspension at specific pH [27]. The flocculation is caused by the neutralization of the OH^- groups adsorbed at basal and edge planes of the platelets [19].

The MoS_2 suspension can be centrifuged and dried. The exfoliated MoS_2 suspension can be almost cleared by using a high speed centrifuge (3600RPM, radius = 15cm) for a sufficiently long time(one hour). However, it is found impossible to completely clear a suspension if the pH is far above the zero charge point (PZC) which is found to be around pH=2 [27]. At higher pH, the MoS_2 slurry obtained in this way is still in a single layer configuration unless it is dried. Therefore, centrifuging at pH>3, decanting the liquid and then adding pure water to recover the suspension enables one to remove ions such as Li^+. For the present study it was found important first to remove LiOH from the suspension and to introduce other ions in solution as desired.

Restacked pure MoS_2 powder is obtained by drying a slurry of exfoliated MoS_2. The just exfoliated or just restacked MoS_2 is believed to be in octahedral coordination when fresh and

upon heating or aging transforms back to trigonal prismatic coordination [28], a form thermally stable up to 1000°C. The slurry can be heated on a regular hot plate at a temperature around 150°C. The X-ray diffraction (XRD) of this restacked dry powder was carried out in the same manner as for as-received MoS_2. It was observed that the restacked dry powder has an identical structure to that of the starting material [26].

Unlike the HOC structure and the inclusion compounds to be discussed later, the air dried suspension is found to have some strongly preferred orientation. Upon drying, the platelets lie with their basal planes parallel to the substrate used (microscope slide) though the orientation is observed to be poorer than that of spreading films (Section 2.5).

2.3 INCLUSION COMPOUNDS

There are numerous ways to prepare inclusion compounds of MoS_2 [29-32]. Emphasis will be given to the methods reported in [31,32], where [31] monolayers of various metal ions are adsorbed on MoS_2 suspended as single layers. The metal ions neutralize the adsorbed OH^- groups. With this technique, a group of inclusion compounds can be formed [31]. XRD measurements were conducted for these compounds in their slurry forms, indicating changes in the inter-layer spacing

for several of these compounds [31], relative to the interlayer spacing in pure MoS_2.

2.4 EVIDENCE OF SINGLE LAYER CONFIGURATION

In the pattern for the exfoliated MoS_2 in suspension (slurry), the absence of the {002}, {103}, and {105} lines is strong evidence for monolayers. The striking agreement between the XRD pattern of exfoliated MoS_2 slurry and the calculated curve for one MoS_2 layer [26] provides further convincing evidence that the MoS_2 slurry is made of single molecular layers [26]. When a weak {002} line is observed, it is thought to be from a small portion of unexfoliated MoS_2 mixed in the exfoliated slurry. From further studies of the configuration of the exfoliated MoS_2 [28], claims have been made that the exfoliated material is in octahedral coordination instead of 2H form (trigonal prismatic), before or not too long (one month) after its restacking.

2.5 FILM PREPARATION

The preparation procedure for making MoS_2 films was initiated by Divigalpitiya et. al. [19]. The basic steps consist of the formation of the film at a water/organic interface and the removal of this film from the interface to a substrate.

2.5.1 Blank MoS_2 films

Single molecular layers of molybdenum disulphide in suspension in water can be collected at the interface between the water and a non-polar (water immiscible) organic liquid. The organic liquid that has been used for making blank MoS_2 films is usually cyclohexane. To produce the film, the MoS_2 suspension is mixed well with the water immiscible organic liquid [19]. This "mixing" is usually done by vigorously shaking the bottle containing the organic and the MoS_2 suspension. It is believed that the OH^- groups adsorbed on the basal planes of the platelets are replaced by the non-polar organic molecules during the shaking because the bondings between these OH^- groups and the inert basal sites are weak. However, those OH^- adsorbed at edge sites remain due to their strong bondings to the polar edge sites. With the basal OH^- groups replaced and edge OH^- groups remaining, the platelets will migrate to the organic/water interface because this is energetically favorable. At the interface, the platelet basal planes are in contact with the organic and meanwhile the edge sites can still be in the water. When the film is formed at the interface, a wet glass slide is inserted into the bottle vertically until its lower end touches the interface. The slide is wet to cover the glass surface with polar water molecules and to form another organic/water interface along the substrate which in turn induces the film to spread. The film at the water/organic

interface climbs onto this substrate (Fig.3). The films are then placed in a fumehood for air drying followed by baking in argon or forming gas (95% Nitrogen, 5% Hydrogen) for a period of 12 h at 220°C - 250°C before various measurements on the properties of such films are made. Such heat treatment removes the water and cyclohexane from the films by evaporation.

2.5.2 Organic inclusion

Organic molecules can also be retained in between the MoS_2 layers. The organic must not be very volatile, if we want to have it stabilized in the films. Cyclohexane was used for samples where the organic was not wanted and styrene was used where we wanted the organic layers to be permanent. The latter was chosen for its immiscibility with water, well defined electrical character (good insulator) and readiness to polymerize [33]. The commercial styrene from Aldrich Chemical Company, Inc. is inhibited with 10-15 ppm 4-TBC. To remove the inhibitor, the as received styrene is filtered through a pipet containing AA 101 activated alumina powder from Alcan. When making films, the filtered styrene was used with the addition of benzoyl peroxide as initiator (less than 1%) to assist the polymerization that follows.

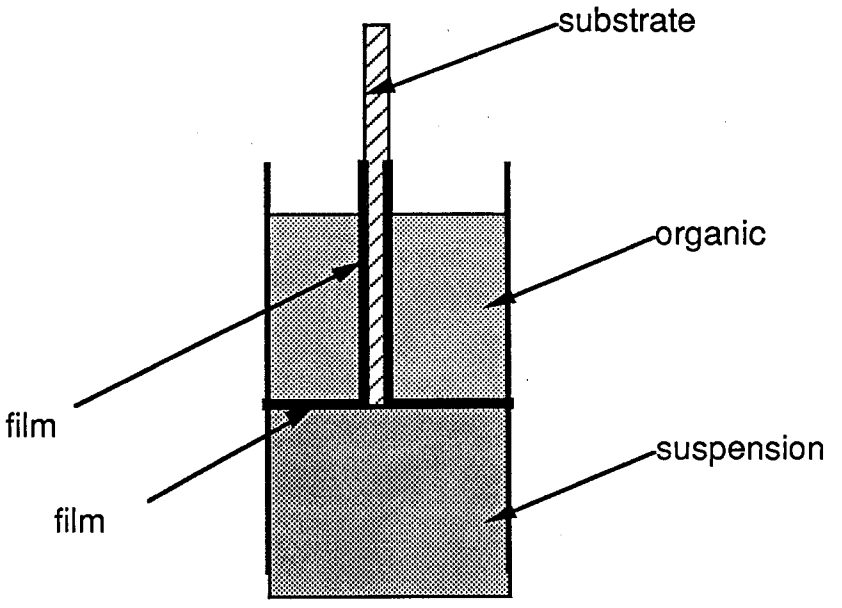

Fig.3 Film formation diagram

2.6 FILM CHARACTERIZATION

Many properties of the films or just exfoliated single layers in other forms have been under extensive studies in our group [19]. The previous work most related to the present study is described below.

The thickness of the spreading films can be changed by various techniques [19]. The thickness mainly depends on the concentration of the MoS_2 suspension used [19], but a pH dependence is also observed. Higher concentration generally results in thicker films and moderate pH (around 7) is preferred for making a thicker sample. The thickness of the films prepared ranged from 30Å to several microns. The optical transparency of the films varies with their thickness, which enables us to estimate the film thickness to a reasonable accuracy. We simply compare by eye the optical transparency of the sample under study with that of a previously prepared film whose thickness is known. Such approximation should yield accuracy in film thickness well within a factor of two. Calibration of this technique was made by using an interference microscope.

The film width is equal to the width of the microscope slide used as a substrate. The length of the films is partially determined by the pH of the suspension used and it was found that a suspension of pH 3 usually yields large area

(long) films [34]. A film, on glass substrate, of more than 10cm long was obtained. The angle between the interface and the substrate also affects the length of the spread film because of the effect of gravity.

Resistivities in directions parallel and perpendicular to the basal planes of the layers were previously measured by using the four point probe and guard ring method respectively [19] and this is the main subject under more careful investigation in this thesis.

CHAPTER III EXPERIMENTAL PROCEDURES USED IN THE PRESENT STUDY

3.1 GENERAL

The basic procedures used to prepare blank MoS_2 films (without additives) were developed earlier [19] as described in chapter 2. To achieve the proposed objectives of this project, some improved techniques have been initiated in order to overcome specific difficulties encountered and to realize desired modifications of the blank MoS_2 films.

3.2 EXFOLIATION

Although a standard MoS_2 exfoliation procedure was established [26], we have optimized some of the steps during our work on the present project. After a prolonged time interval for the Li intercalation, the standard exfoliation procedure has been to wash the Li intercalated MoS_2 with hexane several times to remove the excess Li. It was considered that the H_2 resulting from the reaction between non-intercalated Li and H_2O does not help to separate the MoS_2 layers. We have concluded that such washings may cause de-intercalation i.e. the originally intercalated Li atoms may come out of the van der Waals gaps because of the difference between their concentrations inside and out. Only one (or even no) hexane wash, instead of several, is desirable. When we wash the powder at this stage, we decant the hexane

immediately after the powder settles down. Again this is to prevent the intercalated Li from de-intercalation.

During the reaction between intercalated Li and water, we not only ultrasonicate the suspension as described in the standard procedure but also stir it to provide more assistance to the reaction.

Once the exfoliation process is completed, we allow sufficient time, say 2 hours, for the layers to settle down. Apparently, with the high ion concentration, the layers can "flocculate", but in a form including substantial LiOH, so the material is easily dispersed back to its single layer form in the next step. The next step is to decant the liquid, the LiOH solution, and begin the washing process with distilled water to further reduce the Li^+ concentration.

As in the standard procedure(chapter 2), we have to centrifuge the suspension and wash it several times to remove the LiOH. The centrifuging speed can not be set too high, otherwise the tubes containing the suspension to be washed may be broken. On the other hand, low speed leads to low washing efficiency, as too much liquid remains in the slurry. It is found useful to ultrasonicate the suspension after each water wash to well expose the Li^+ trapped between MoS_2 layers.

3.3 METAL ADDITIVES TO RESTACKED MoS_2

Metal ions can be placed at either edge planes alone, or both basal and edge planes of the platelets. The latter, where enough metal ions are provided to cause flocculation, yields inclusion compounds where the metal ions connect neighboring basal planes and may cause massive circuit shorting as with metal intercalated MoS_2 single crystal [4] in resistance measurements in the direction perpendicular to the layers. Such inclusion compounds are discussed in Section 3.3.1. We have found the former makes sort of bridges along the layer boundaries as will be discussed in Section 3.3.2.

3.3.1 Metal inclusion compounds

Metal ions when added in appreciable amounts to an originally somewhat neutral solution will cause the MoS_2 suspension to flocculate as a powder with the metal ions trapped between the MoS_2 layers as discussed in section 2.3. This powder can be viewed as alternating MoS_2 and metal hydroxide sheets, a sandwich-like-compound, but these small particles (sandwiches) have very different orientations and the technique to align them in order to make uniform large area inclusion films has not been developed yet, though metal atom insertion into a MoS_2 single crystal was reported a long time ago [4]. In our study, such flocculation is undesirable because particulates, produced by flocculating can appear in the film to be studied, and are imperfections.

As discussed later, we have been interested in Cu^{++}, Ni^{++} and Co^{++} additives to the MoS_2 platelets. Earlier studies [31] showed inter-layer spacing changes with inclusion compounds using Ni^{++} and Co^{++}. We have observed a spacing expansion with a Cu^{++} included compound (MoS_2 layers as host) by using XRD. This Cu included compound is obtained by adding $Cu(NO_3)_2$ solution to the MoS_2 suspension to cause flocculation. The inclusion system of organic molecules in restacked single layer MoS_2 [32] will be discussed in some detail later.

3.3.2 Metal bridges

In our studies, we were interested in adding metal ions to the edges of the platelets to act as "bridges" to aid the transfer of carriers from one platelet to another.Solutions of metal compounds {viz. $CuCl_2$;$Cu(NO_3)_2$; $CoCl_2$; $Co(NO_3)_2$; $NiCl_2$; and $Ni(NO_3)_2$} with a concentration before mixing of 10^{-2} M are mixed (individually) into the MoS_2 suspension during the process to make spreading films. The pH of the MoS_2 suspension used was 7 (which, after mixing with the additive solutions, is reduced to around 5), well above the Point of Zero Charge, PZC (pH=2) to avoid flocculation. The solution is added gradually because it is found that a local surplus will cause local flocculation which in turn makes it difficult or even impossible to obtain quality films. On the other hand, insufficient supply of these metal ions results in trivial or

non-detectable effects. The maximum concentration of the desired material is limited by the flocculation point which depends on the pH and concentration of the MoS_2 suspension as well as the concentration of metal ions being added. Once the films are formed with metal additives around the platelet edges (as will be discussed in Chapter 4), they were subjected to the same thermal treatment to eliminate water and organic (where in appreciable concentration) trapped in between the MoS_2 layers. The existences of these metal bridges are confirmed by Scanning Electron Microscope (SEM) (Tables 2, 3 and 4). The data and the resulting effect on the properties of the film are discussed in chapter 4.

One can imagine that the effects of these metal additives will depend considerably on their concentrations. Different solutions of different concentrations were used to study such dependence. We vary the concentration by adding different amount of the solutions of the additives. The concentrations determined this way should be proportional to the concentrations of these additives in the films at large. It is possible to determine the additive concentrations to higher accuracy by using SEM, but we think it unnecessary for qualitative analysis.

3.4 STYRENE INCLUSION

Many organic solvents that are water immiscible can be used to prepare the spread films [32]. Styrene was chosen mainly because of its interesting electrical characteristics before and after polymerization.

3.4.1 Filtering the styrene

The commercial styrene ($C_6H_5CH=CH_2$) contains an inhibitor to prevent the styrene monomers from spontaneous polymerization. The inhibitor must be removed since we need to eventually polymerize the monomers. The styrene was filtered through a long pipet containing activated alumina powder. It would take a long time for the styrene to diffuse through the long pipet, increasing the chance that the styrene monomers polymerize spontaneously because now the inhibitors are removed (although such effect may be negligible). It was observed that filtered styrene will polymerize spontaneously if placed at room temperature in open air for days. To speed up the filtering process, high pressure air is passed through the pipet. The presence of oxygen (in the air) makes the spontaneous polymerization less likely. The filtered styrene is kept in a refrigerator if not immediately used, however, we found that the freshly filtered styrene is better for making uniform films. The filtering process must be carried out in a fumehood because the styrene vapor is highly toxic.

3.4.2 Double modifying

The metal compounds (in solutions) mentioned earlier can still be added when the organic solvent used is styrene instead of cyclohexane, and this allows the edge plane sites as well as the basal plane sites to be modified simultaneously in an attempt to enhance the electrical anisotropy of the films.

The selection of the organic solvent is observed to have some influence on the film formation. For the same MoS_2 suspension, the use of cyclohexane or styrene results in different lengths of films, even different thicknesses and uniformities. For example, with the same suspension we usually obtain longer, thinner and more uniform films when cyclohexane is used. Also, the maximum addition of the metal compound solutions also differs between these two cases. Generally, cyclohexane is easier to deal with. Larger amount of metal additives can be used with cyclohexane as the solvent and longer films can be obtained. Such observations are thought due to the different efficiencies of replacing the OH^- groups on platelet basal planes by different organic molecules. This is the reason why we choose cyclohexane as the water immiscible solvent when organic inclusion is not needed.

3.4.3 Drying

It has proved to be a delicate procedure to dry the styrene included films for they cannot be heated at the temperature we treat the inorganic films (MoS_2 only or just with metal additives). Styrene included films are placed in a desiccator when the styrene is still in monomer form. This presumably removes some of the water molecules from the film while not affecting the styrene monomers very much. Once the styrene monomers are polymerized (see Section 3.4.4), they can stand higher temperature. The films, after the polymerization of the included styrene, can be put into a high vacuum (10^{-7} torr) at 80°C (the temperature is maintained by applying a current through the evaporation boat to which the films are attached) to further dry the film. Polystyrene should not evaporate even at high vacuum. The heating temperature is so chosen that on one hand it favors the evaporation of water molecules and on the other hand avoids decomposition of the polymer.

3.4.4 Polymerizing the styrene

We found that it is much more difficult to polymerize the styrene molecules, in the form of a sheet of one molecular layer thick trapped in between the MoS_2 layers, than to polymerize bulk styrene. In fact, what is happening when we "polymerize" such styrene sheets is not clear, as discussed in section 4.4.4. Benzoyl peroxide (BP, less than

1%) is used as thermal initiator for the polymerization. The initiator is added just before making the film, i.e., just before shaking the bottle which contains MoS_2 suspension (lower phase) and filtered styrene (upper phase). The films, after being in a desiccator for hours, were placed in a bottle, sealed by rubber cover. The bottle was flushed with dry nitrogen (N_2) for 15 minutes. This removes the air that was originally in the bottles for, as mentioned before, the O_2 in air will react with the initiator at high temperature and make the styrene polymerization very unlikely. The bottle was tightly sealed to keep the N_2 in and maintains a significant styrene vapor pressure while heating. The bottle containing sample films was then placed in a furnace and the temperature is raised slowly to 60°C. A small bottle containing only filtered styrene with the proper amount of initiator (BP) is placed beside that with sample films. This small amount of styrene serves as a reference. When the bulk styrene is polymerized (usually after overnight), the styrene sheets in the films are expected to be polymerized as well. The styrene vapor pressure in the film-containing bottles, presumably keeps more styrene monomers in the films from evaporating before the thermal polymerization takes place.

UV polymerization method was attempted but without success. The initiator used for this attempt is an optical initiator instead of BP (thermal initiator). X-ray

polymerization was also attempted inside the sample chamber of the X-ray diffractometer, and was again, unsuccessful.

3.5 FILM CHARACTERIZATION

The characterization of the films is relatively easy, compared to their preparation, except for a few technical difficulties. It should be stated in advance that the characterization presented here is only qualitative for reasons to be discussed.

3.5.1 Thermal stability

Many physical quantities of the semiconducting films will, of course, be temperature dependent. However, only a very limited thermal stability study was conducted at moderate temperature (200 - 250°C). In general a thermal treatment at about 220°C was applied to dry the inorganic films and resistivity measurements were made at room temperature.

3.5.1.a Blank films

Although, 2H-MoS_2 is reported to be stable up to 1000°C [1]. The inorganic films were baked in argon atmosphere at a temperature not higher than 250°C to remove water and organic molecules. In addition, we found that the temperature must be raised slowly from room temperature to the desired value. Both rapid heating and rapid cooling at this stage could

probably cause destruction of the high orientation of the MoS_2 platelets, i.e., create defects in the films which in turn may affect the properties of the films. From XRD patterns (Fig.4 - 5) (the broad bump between 20° and 30° is due to the substrate), we believe that the above thermal treatment does not distort the film orientation but just drives out the water and undesired organic molecules from between the layers of the films.

Fig.4 - 5 indicate very high orientation of the platelets when they form a film, as the only dominant lines are the sharp {00ℓ} lines. The position of the peaks in the XRD patterns provides a way to calculate the inter-layer spacing along the direction normal to the layers in the film by simply using the Bragg equation.

3.5.1.b Metal bridging films

Metal bridging films can stand the same thermal treatment as blank films because the metal compounds, initially in the forms of hydroxides, are thermally stable, at least to the temperature of dehydration. After dehydration they should be stable at any reasonable temperature. XRD does not show any visible changes in the patterns after the baking treatment. However, we suspect the metal hydroxides may dehydrate into their corresponding oxides for reasons to be analyzed in chapter 4.

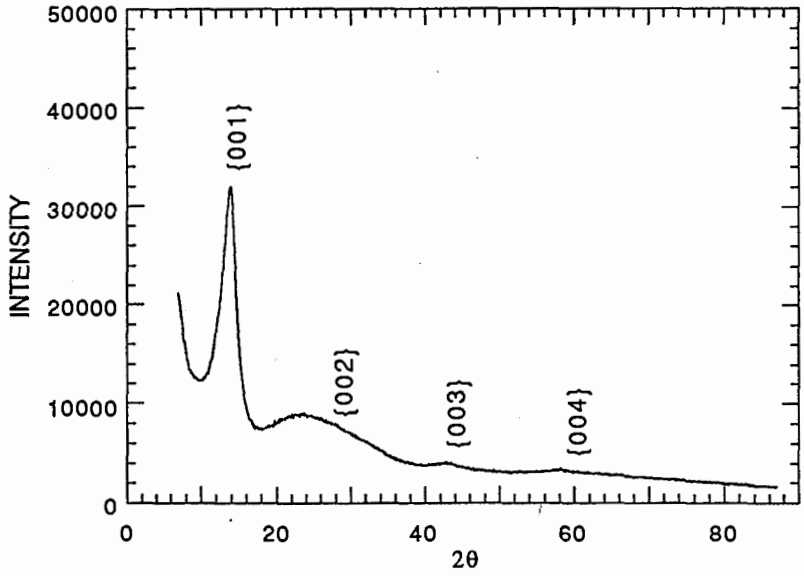

Fig.4 X-ray diffraction pattern of a blank film

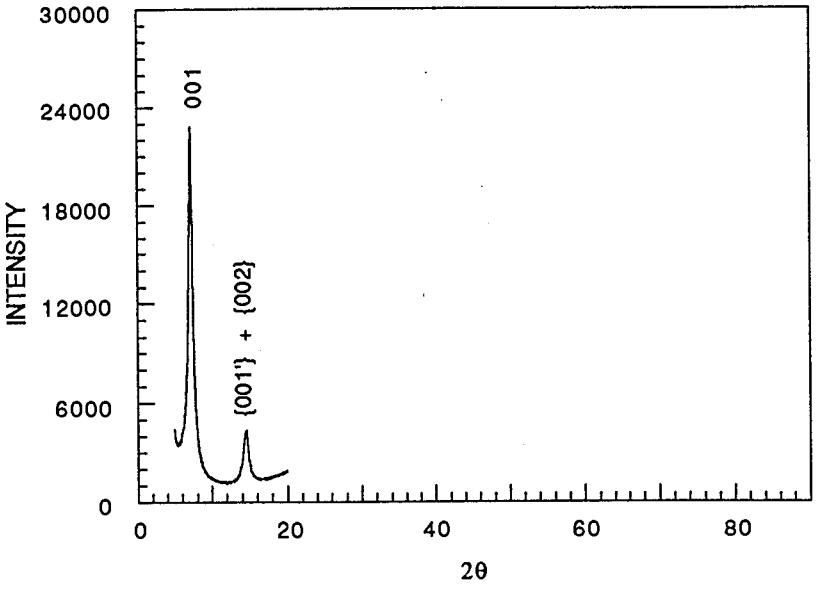

Fig.5 X-ray diffraction pattern of a polystyrene included film. The {001} peak is due to phase 1 (organic sandwich). The {001' + 002} peak is due to {001} of phase 2 (pure MoS_2) and {002} of phase 1 overlapping.

3.5.1.c Organic/inorganic composite films

The thermal treatment of those films containing styrene calls for extra caution as discussed in detail in Section 3.4.4. Styrene molecules, even after polymerization, are best restricted to a temperature less than 100°C, because at higher temperatures the polymer can decompose and evaporate. Following the polymerization at 60°C, instead of being baked at 220°C, the samples were transferred into a vacuum of 10^{-6} torr and heated in the vacuum at 70-80°C to further dehydrate the samples while avoiding decomposition of the polystyrene.

3.5.2 Inter-layer spacing

Inter-layer spacings have been determined by XRD in this study. The interlayer spacings of various film samples can be calculated from the their XRD patterns and provide valuable information on the inclusion of additives between the basal planes of the layers.

XRD patterns were obtained with a Philips diffractometer using Nickel-filtered Cu K-α radiation. The current and voltage were chosen as 35mA and 45kV respectively for all the XRD measurements done in this work. The diffraction pattern for untreated 2H-MoS_2 powder (the starting material) is shown in Fig.6.

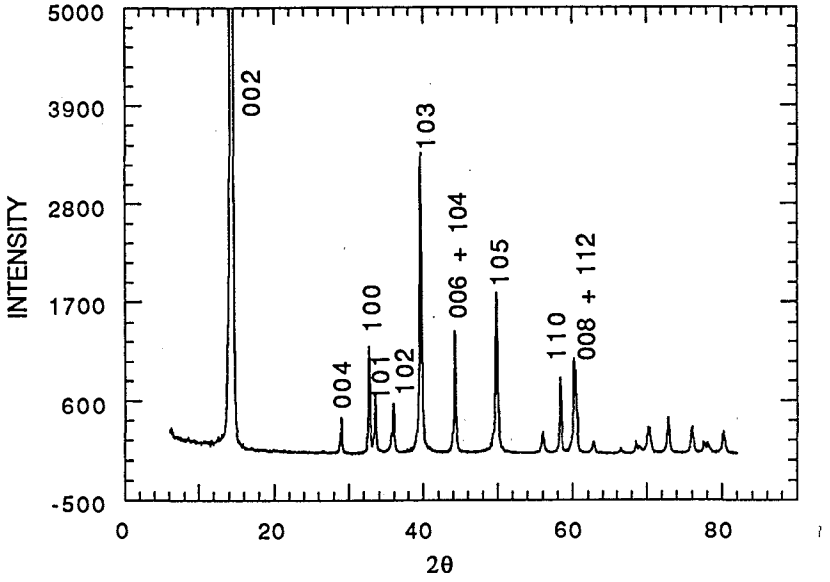

Fig.6 X-ray diffraction pattern of as-received 2H-MoS_2 powder.

By centrifuging the suspension of exfoliated MoS_2 single layers, decanting the liquid, and washing it with distilled water (3-5 times), a slurry of exfoliated MoS_2 in water can be obtained. The concentration of such slurry is adjusted such that the slurry can remain in the XRD sample holder as the sample holder is rotated in a vertical plane. On the other hand, the slurry should be dilute enough to avoid undesired drying (restacking). It has been found [26] that the resulting XRD pattern closely resembles the calculated pattern for single layers of MoS_2 , and this technique has been valuable to indicate successful exfoliation into single layers.

3.5.3 Determination of carrier types

The original MoS_2 powder is a p-type semiconductor. The carrier type can be adjusted by adding different impurities as has been clearly demonstrated with inclusion compounds [31]. The metal bridging films also show such changes but less significantly compared to those with inclusion compounds because the concentration of impurities is much much lower in the former.

A piece of commercial silicon wafer whose carrier type is known was used for calibration. We used a voltmeter to measure the voltage across two points on the wafer. Of course, when both electrodes are at the same temperature, one

observes a zero voltage. However, when a temperature gradient is created by heating the wafer at one electrode by placing the tip of a hot soldering iron near this electrode, a voltage can be read, positive or negative depending on the carrier type of the silicon wafer. Then the same procedure is followed with the film samples under examination. From the sign of the voltage we can infer the majority (may have electrons and holes at the same time) carrier types of these semiconducting films.

3.5.4 Resistivity

The electrical anisotropy of the MoS_2 is partly characterized by the resistivity difference between that in the direction parallel to the basal planes and that perpendicular to the basal planes. Again however, most previous work was done on single crystals of MoS_2. The polycrystalline nature of our films drastically modifies the MoS_2 conducting property as will be shown later.

3.5.4.a Conducting substrates and contacts

To make the resistivity measurements in the direction perpendicular to the layers, a conducting substrate is needed. Another electrode is evaporated on top of the film after all appropriate treatments, or one can use silver DAG directly. To make a conducting substrate, a 200Å thick layer of Au, Al, or Ag was evaporated onto a glass slide and

tested. It was found that Al coated substrates were undesirable due to high contact resistance between Al and MoS_2. Au was also unsatisfactory as the coating metal for it tends to peel off when in water. For our purpose, the Ag coating provided satisfactory contacts. The reported ohmic nature of the contacts [14] is confirmed by the perfect linear relation between **I** and **V** of a two point probe measurement (Fig.7) with **V** varying from 1mV to 2V, and a observed fact that $R_{2pb} = R_{4pb}$ for the same sample, where R_{2pb} is the resistance measured with a two-point-probe method and R_{4pb} four-point-probe.

3.5.4.b Transferring technique

The Ag coated glass substrates are not water wettable, therefore they cannot be used to spread films directly from a water/organic interface. A so-called transferring technique as shown in Fig.8, was developed to solve this problem. The conducting substrates are supported in a big beaker containing distilled water, then the water surface level is adjusted by adding or removing water from the beaker until the substrate is just under the water surface. Films are prepared in another beaker by the standard spreading techniques. The freshly formed spread films, before they are completely dry, are very slowly inserted vertically into the water by adjusting the jack. The film on the glass slide will peel off and float on the water surface as shown in Fig.8.

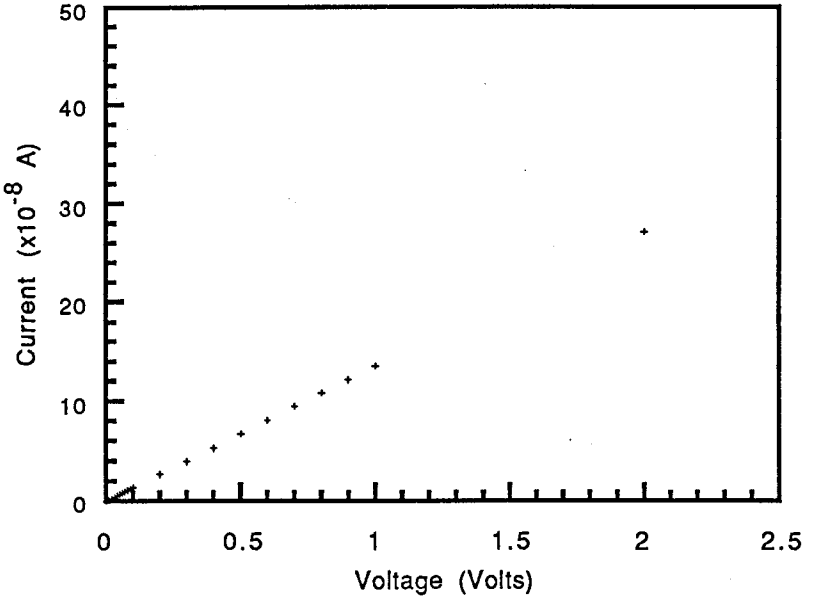

Fig.7 Two-point-Probe resistance measurement on a Ni^{++} added film.

sample dimensions: 2.5cm(width) by 0.5mm(length) by 300Å(thickness)

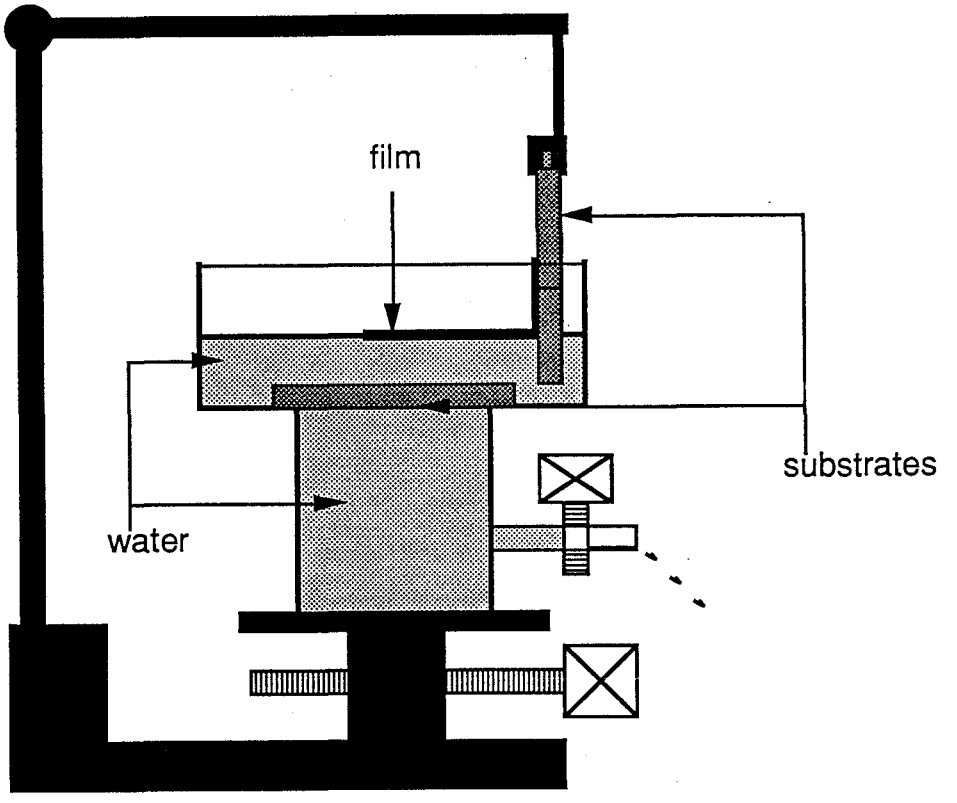

Fig.8 Film transferring setup

The surface level is then lowered by slightly open the valve until the conducting substrate barely emerges. The film is therefore transferred onto the previously buried conducting substrate and ready for further treatment. The transferring must be done very carefully and slowly otherwise the film may break into pieces when being returned back to the water. If this is done properly, in principle, one should be able to maintain the quality of the original film. Multiple films made by repeatedly using the transferring technique (with the film dried after each transfer) are thought to possess the same properties as a single film except a larger thickness.

A more direct technique to form a film over a Ag contact was by using small contacts that the spreading film will cover by "inertia". It is very difficult to get a film on top of a conducting substrate via direct spreading since, as we said, the conducting substrates are not water wettable. The reason that a wettable substrate must be used, as discussed in chapter 2, is that we must provide a water/organic interface for the film to spread on. A wet glass slide dipped into the organic (upper phase) layer serves this purpose (Fig.3). However, if the glass slide is only partially covered with metal (Ag), [say, 10% of its area(Fig.9)], such that most of the substrate surface can still be wetted. Then the film at the interface will climb up along such a

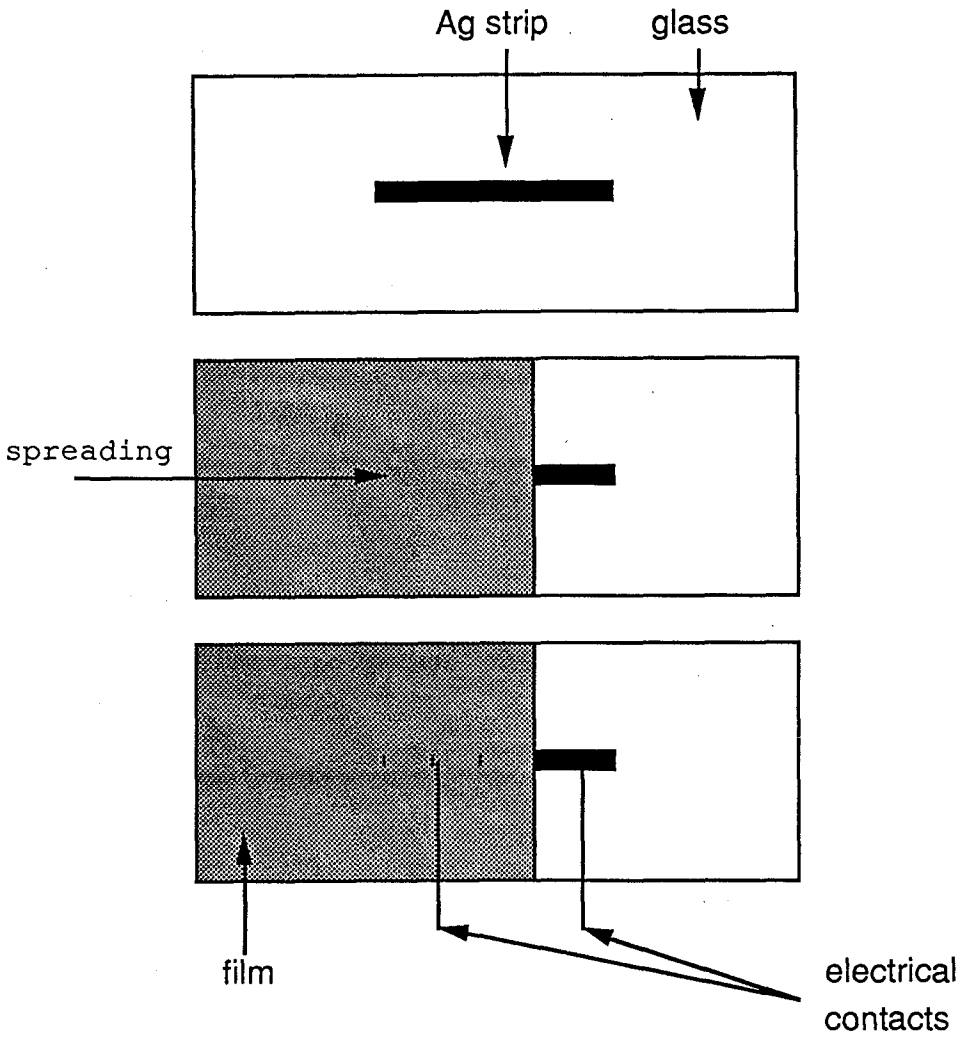

Fig.9 Direct spreading diagram

substrate and because the film of platelets is in motion, it will have to mechanically (not energetically) cover the small metal strips on the substrate.

It was also found that a water layer may stay on a very clean Ag coated glass for a short while and in such "rare" cases we could let the film at the interface directly climb along the substrate now that this conducting substrate is wet. We did not investigate this phenomenon.

After any of these procedures, metal spots can be evaporated or silver DAG applied on top of the film, to make the top contacts. Fig.9 indicates the deposition of electrical contacts for measuring resistivity $\rho_{\perp}$ perpendicular to the layers, when the film is prepared by the "inertia" technique. The film covers the Ag strip as discussed above, then contacts are deposited over the film for a two-point resistance measurement.

3.5.4.c Four point probe and guard ring masks

A four point probe and a guard ring mask were designed to make the resistivity measurements parallel to and perpendicular to the layers respectively. The masks were made of Cu sheet. The patterns for these masks are shown in Fig.10. The reason for making such masks is to make identical electrical contacts to samples. Also, the use of these masks

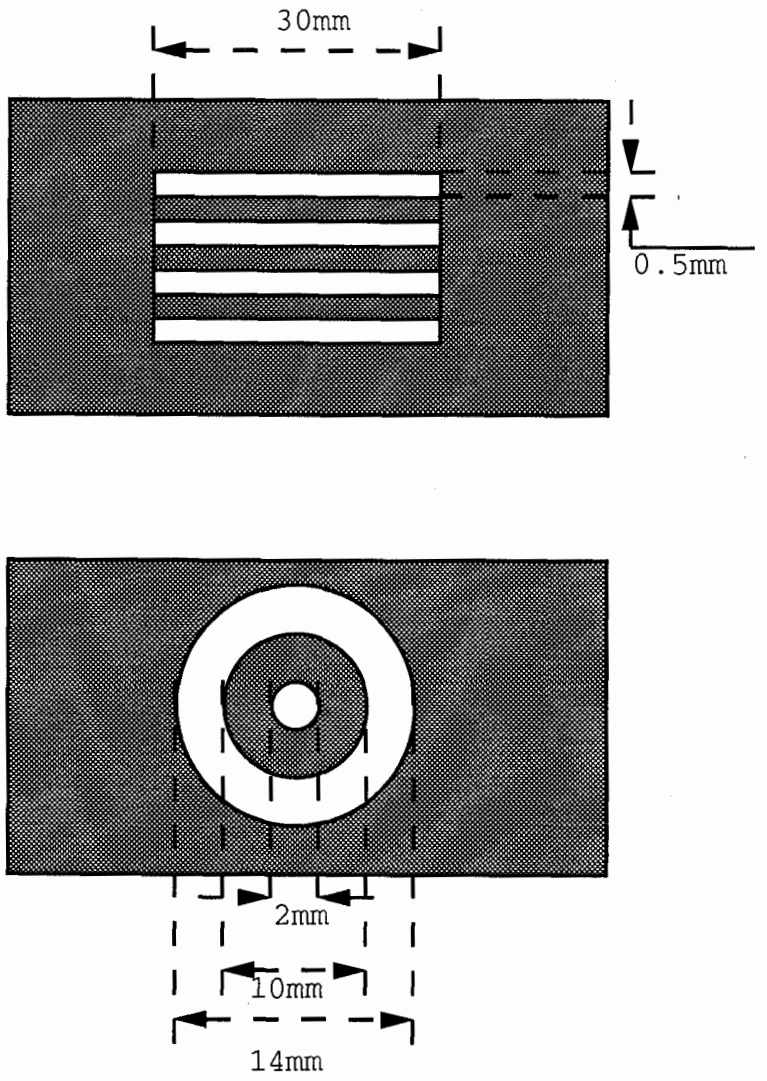

Fig.10 Four-point-probe and guard-ring masks

(not drawn to scale)

reduces the difficulty of manipulation in evaporating the top contacts on the films because the thin film can be very easily damaged, and (although not shown) the design of the masks avoids direct contact between the film and the mask. However, we found that the guard ring method conventionally used for measuring c-direction resistivity of single MoS_2 crystals is not needed (see appendix) in our case. One observes no difference when the ring is used or not probably because of the polycrystalline nature of the films and the small dimensions of each platelet.

When preparing samples for resistivity measurements parallel to the layers, scratches were made with a needle along the planned boundaries of the Ag strips before the evaporating. This is an additional measure to ensure that the Ag electrodes are in contact with every layer of the film. However, it has been argued that the measured parallel resistivity is the bulk resistivity (not just that of the top layers) even with the electrodes on top of the film surface only.

3.5.4.d The measurements

A DC power supply(6215A HEWLETT *hp* PACKARD POWER SUPPLY), a multimeter(177 KEITHLEY MICROVOLT DMM) and a electrometer(616 KEITHLEY DIGITAL ELECTROMETER) were used to make the resistivity measurements in directions parallel or

perpendicular to the layers. The circuits for these two kinds of measurements are shown in Fig.11 and Fig.12. The results will be presented in the next chapter. The reason to use the four probe method to measure the resistivity in the plane is to eliminate the effect of contact resistance at points B and C (Fig.11). However, two probe measurements on those same samples (with Ag as electrodes) show almost identical values with voltage varying from 1mv to several volts, which indicates that the contact resistance in our case is indeed negligible (Fig.7). The use of the guard ring method is to force the current to go directly through the films instead of spreading along the longitudinal dimension. However, the sample films we used have an very small thickness (~300 Å) and platelets have small lateral dimensions. The resistivity in the direction parallel to the layers is also fairly high (as will be given in Chapter 4). Because of these factors, the guard ring was found to have no effect. We can conclude negligible spreading of the current occurred. A model is discussed in the appendix. In later measurements, we simply deposited many dots of Ag on the top surface of the film as contacts assuming negligible enlargement of the effective conducting section area over the area of the dot. The advantage of the multiple dot structure is that by doing so we were able to find pin-hole free areas for the measurement. The ways to check whether or not there are pin holes in the area of interest include optical microscope examination or

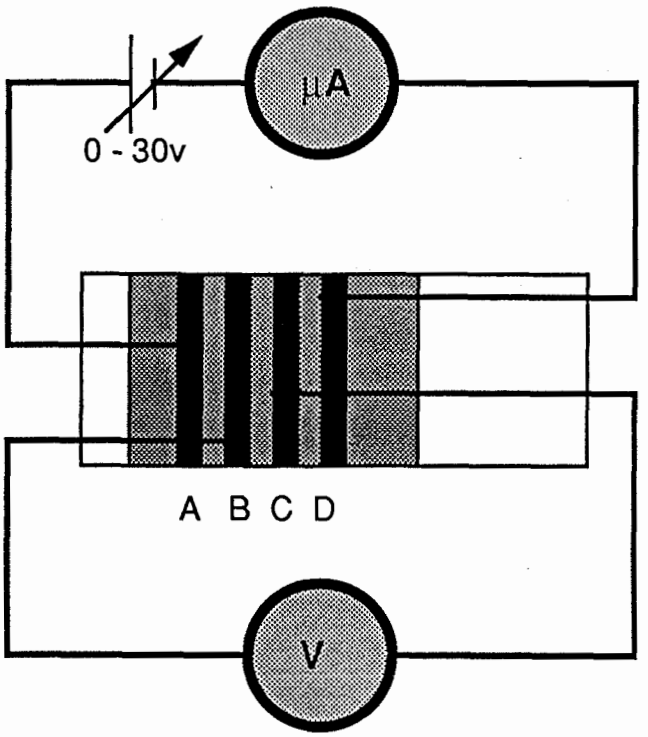

Fig.11 Parallel resistivity measurement setup

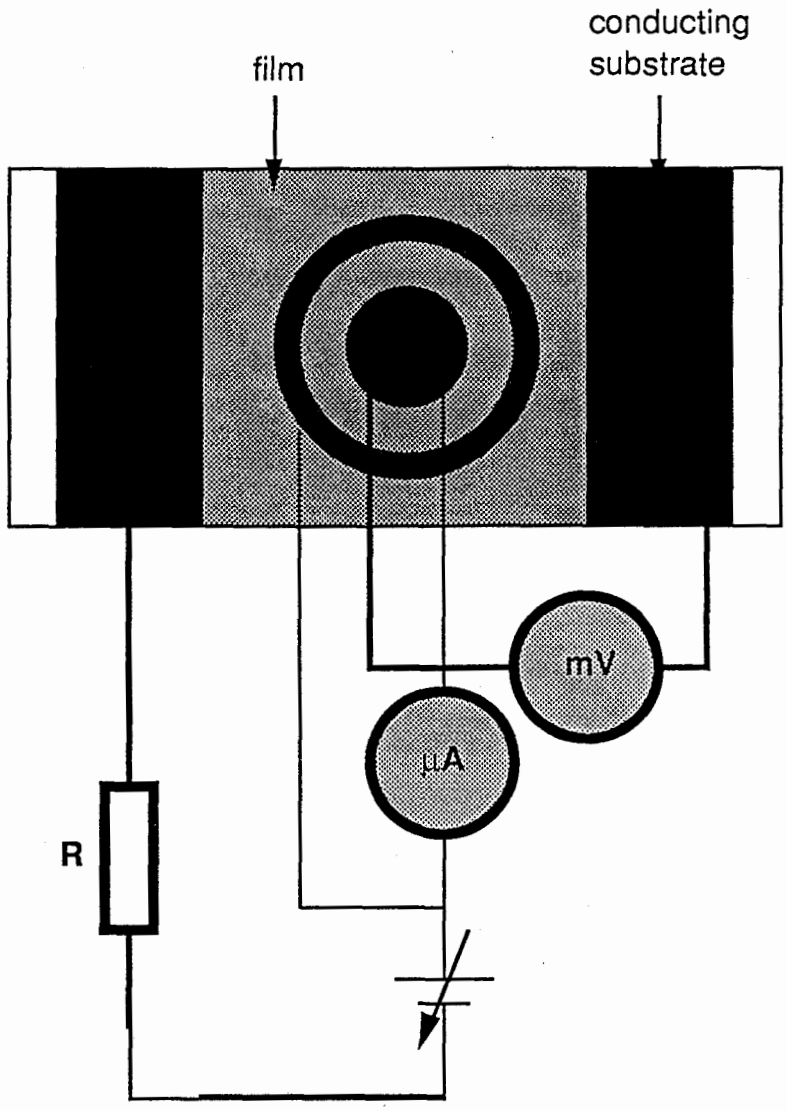

Fig.12 Perpendicular resistivity measurement setup

simply putting a beam of light (a laser is best) through the sample to see if and from where there is any leakage onto a screen.

3.5.5 Temperature dependence of conductivities

The temperature dependence of conductivities in the two characteristic directions of a film was studied to determine the activation energies in these directions and further infer the routes taken by the current carriers when a voltage is applied in the direction perpendicular to the layers. It was of interest to ascertain whether the electrons directly jump over the van der Waals gaps or detour around the boundaries of the platelets.

The circuits to measure the temperature dependence of the conductivity in either of the two characteristic directions are the same as those used earlier (Figs.11 and 12) for measuring the film resistivities at room temperature in open air. However, the samples now are placed inside a quartz tube through which Ar flows and the tube is placed inside a furnace. We pass Ar through the tube to avoid possible oxidation of the films when the furnace temperature is high. The furnace temperature was monitored by a built in thermocouple and an additional thermometer fixed to the sample. Wires were attached to the sample film inside the tube through a three way connector. We allowed sufficient

time for the system to reach the desired temperature and then thermal equilibrium, say, two hours for each reading. We started the experiments at room temperature and increased the temperature slowly. After the data acquisition is completed, the furnace power supply is turned off to allow the furnace to slowly cool down back to room temperature and re-measure the room temperature conductivity of the same film. We find the room temperature resistivity is the same as it was before the heating. One should understand that the low temperature activation energy for such films may be different from what we present in Chapter 4, as is known to be the case for single crystal [14].

Organic sandwiches always call for extra caution and the temperature dependence experiments have not been done on such samples.

CHAPTER IV RESULTS AND DISCUSSION

4.1 FLOCCULATION

Studies were made to clarify the role of ions in inducing flocculation. The study was needed because our approach was to introduce ions into the suspension and for film preparation, flocculation is of essential importance.

We have found exfoliated MoS_2 layers may stay in suspension for up to months if the suspension is in moderate pH (around 7, say). This is because the platelets are surrounded by OH^- groups [19] which in turn are neutralized by protons and/or other cations in solution. This forms double layers around the MoS_2 platelets. The (double layer)/(double layer) repulsion will keep the particles away from each other. If the ion concentration is high, as with the original LiOH produced, flocculation can be induced, as is known in the literature [38] because the double layer collapses. When the pH of the suspension is reduced, the OH^- adsorption is also accordingly reduced and it was found that at about pH = 2 the suspension will flocculate rapidly, hence, the pH 2 is thought to be close to the PZC for such system. Other positively charged particles (than H^+) can also cause flocculation by adsorption, where the OH^- reacts with the ions to form the hydroxides. The metal ions that we want to include adsorb thus, as mentioned earlier when discussing the

metal bridge modifications. The flocculation restricts adjusting the suspension pH freely in our studies.

4.2 HIGHLY ORIENTED SYSTEM

The spreading layers obtained with the methods described in Chapter 3 form a highly oriented system (polycrystalline film). This is confirmed by the XRD patterns for such films(Figs.4 and 5). The formation and resulting orientation of these films are discussed in reference [19]. The position of the {001} peak, which reflects the inter-layer spacing, depends on the incorporation of moisture or other foreign species, and this is used [32] to determine the separation of the basal planes of the MoS_2 platelets due to those added species.

Blank MoS_2 films have a inter-layer spacing of 6.15Å (separation between two neighboring Mo layers) which is the same as in bulk MoS_2 powder (Fig.6), however, if the XRD is conducted while the films are wet, we might be able to see a larger spacing due to the existence of moisture (water double layers) and organic molecules. This is reflected by a shift in the position of the peak corresponding to the 6.19Å spacing.

No spacing change was observed by XRD for metal included films. This can be compared to such shifts for included

metals (on the basal planes) (see reference 31 and Section 3.3.1) and may indicate that in our case the metal elements are indeed at the edge sites, not the basal sites. The observation is in agreement with the model of Divigalpitiya et al [19] who concluded that in the film-forming process the organic displaces the OH^- ions from the basal plane, and so leaves no sites there for attraction of metal ions.

With the styrene molecules present, either in monomer or in polymer forms, a substantial shift of the {001} peak can be observed and this shift characterizes the size of the molecules inserted into the MoS_2 inter-layer gaps [32]. One fact is that we always observe the {001} peak of blank films together with the {001} peak of the organic sandwiches (Fig.5). This clearly shows that such organic sandwiches in fact consist of two phases, namely, one with organic in the van der Waals gaps (phase 1) and the other without (phase 2). We have not succeeded in formulating a sample with only one phase, a pure organic "sandwich". The intensity ratio between {001,phase 1} and {001,phase 2 + 002,phase 1; "overlapping"} has varied from 4:1 to 2:1 in our measurements, depending on the degree of success in styrene inclusion and polymerization. The ratio reflects the proportion of these two phases and this ratio changes (reduced) significantly after the styrene polymerization if the polymerization is not done satisfactorily as the styrene monomers evaporate.

4.3 THE CHANGE IN CARRIER TYPE

The metal bridging films show clear signs of carrier type changes. It was observed that the Cu^{++} bridging film is a p-type semiconductor (more p-type than the blank films) while Ni^{++} and Co^{++} bridging films were both n-type.

As described in Chapter 3, with the inclusion of various elements, the carrier type of the starting material (2H-MoS_2) can be changed (originally p-type). These changes result from the interactions between the host material and the inserted species. The changes in inter-layer spacings with the Ni, Co, Cu included compounds are indications of such interactions. The energy levels of Ni^{++} and Co^{++} are presumably higher than the Fermi energy of MoS_2 and hence electrons will be donated to the host and therefore make the film n-type (Figs.13). On the other hand, the energy levels of Cu^{++} is presumably lower than the Fermi energy of MoS_2 and electrons flow from the host to orbitals of Cu and make the film more p-type (Fig.14). The situation at the platelet edges could also be described as follow: there exist some "edge" state. The energy associated with such state is presumably lower than that of the electrons occupying the outmost orbital of Ni^{++} or Co^{++}, hence, the electrons move to this "edge" state (electron injection from Ni^{++} or Co^{++}). On the other hand, the "edge" state energy is presumably higher than that of (an) empty orbital(s) of Cu^{++}, hence, electrons move to such empty

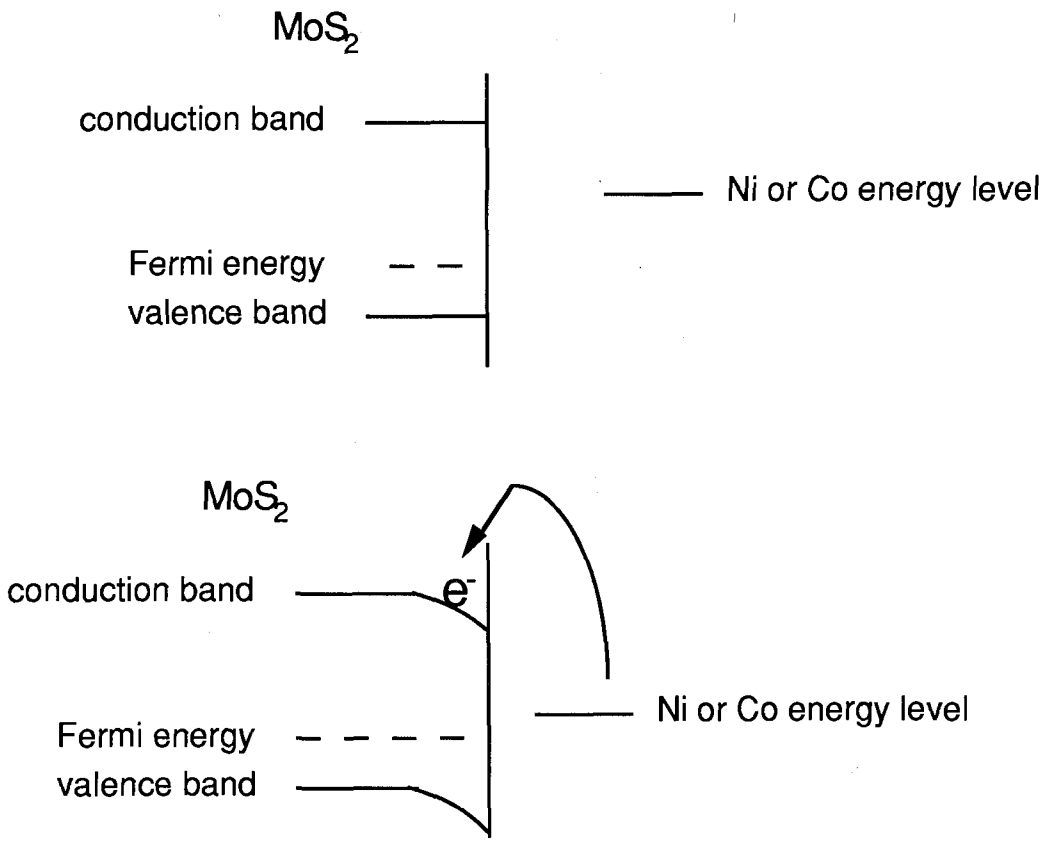

Fig.13 Band model for Ni or Co included film

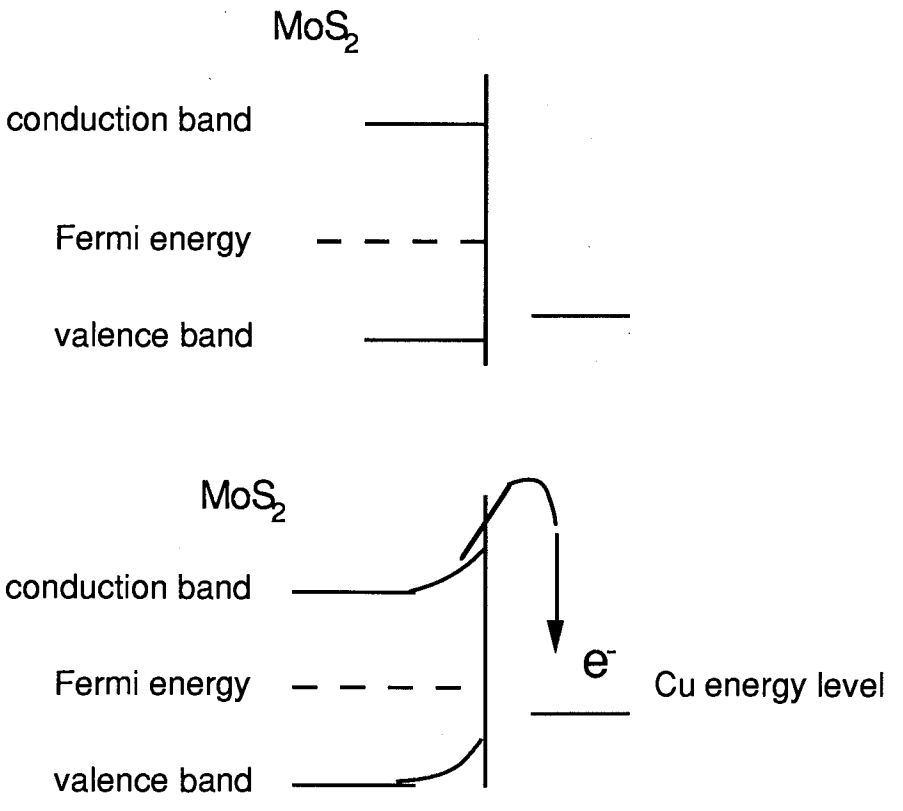

Fig.14 Band model for Cu included film

orbital(s) (electron injection to Cu^{++}). Since the additive ions may appear around the platelet edges in forms of , for example, $Ni(OH)_2$, $Ni(OH)^+$, NiO, or even Ni and there are Mo and S involved, it is very hard to present a more detailed picture of the energy bands at the edge sites based on the information we collected. The actual mechanism of the interactions between the layers and the additives is not clear and the effects of such interactions can not be explained quantitatively and accurately at the present stage. Again, we are dealing with a much smaller amount of additive than that present in an inclusion compound.

It is suggested, however, that the carrier injections at the edges of the platelets cause these changes in carrier type. As discussed in Section 4.2 metal ions are present only at the edges of the platelets. When, as in Fig.13 and Fig.14, the metal additives around the platelet edges inject carriers (electrons from Ni and Co; holes from Cu) to the host material, they form conducting rings with different properties from those of the "bulk" material. The Ni or Co included films have n-type rings around their platelets while remaining p-type inside the rings and similarly Cu included films have relatively strong p-type rings whilst remaining relatively weak p-type within such rings. The suggestion that strong p-type rings are formed is based on the high conductivity in the presence of copper, discussed in Section

4.4 below. As frequently stated, the boundary behavior dominates the film properties, hence, these characteristic rings give us those strong signals of changes in the carrier type from that of a blank MoS_2.

4.4 ELECTRICAL ANISOTROPY

The electrical anisotropy of a single MoS_2 crystal is due to its structural anisotropy, i.e., the weak inter-layer interaction and strong interaction among atoms within a layer. The high electrical anisotropy achieved here (given in Table 1) is a result of combining the original electrical anisotropy with the effect of the metal bridges and the effect of the polystyrene insulating layers.

Fig.15 shows a set of typical data from a $\rho_{//}$ measurement with various voltages applied. Table 1 gives a summary of the observed resistivity values with and without metal ions (introduced as in Section 3.3.1). the results with no additives are discussed in Section 4.4.1 and the results with metal ions in Section 4.4.2.

The thickness used to calculate the resistivity was estimated to be about 300Å by comparing the optical transparency of the sample films with that of a film whose thickness was known (as described in Chapter 2). The calibration was made by measuring (using an optical

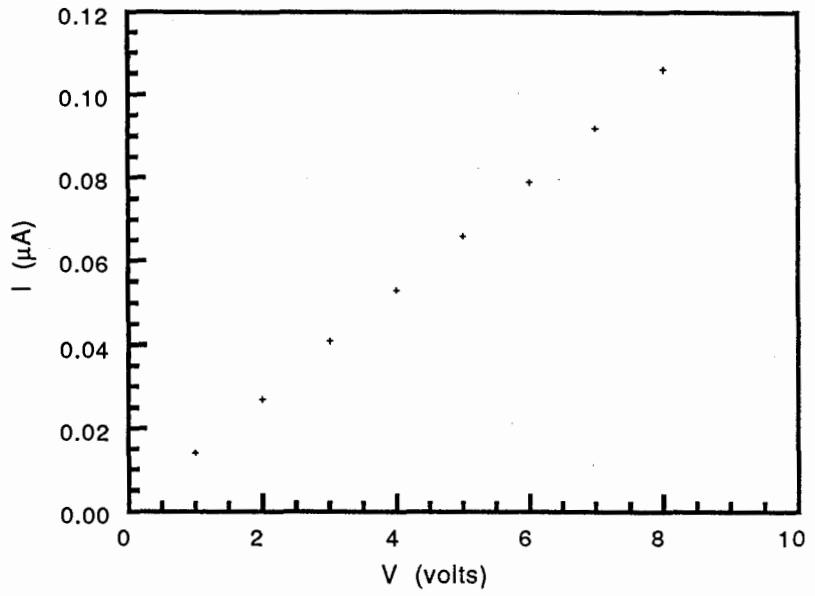

Fig.15 I vs V for blank film $\rho_{//}$measurement. $\rho_{//}$ is the resistivity in the direction parallel to the basal planes ($\rho_{//}$) of a blank film (refer to Fig.11). The dimension of this sample is the same as in Fig.7:

2.5cm(**w**) by 0.5mm(**l**) by 300Å(**t**)

Table.1 Carrier types and resistivities* of inorganic films

	carrier type	$\rho_{//}$ (Ω.cm)	$\rho_{\perp}$ (Ω.cm)
single crystal	p	10^3**	10^5**
blank film	p	10^4	$2x10^6$
Ni^{++} containing***	n	$5x10^2$	$3x10^6$
Co^{++} containing***	n	$8x10^2$	$8x10^5$
Cu^{++} containing***	p	$6x10^2$	$2x10^6$

* the measured values from sample to sample varied up to a factor of 2 from the values indicated

** reports give $10-10^3\Omega$.cm for $\rho_{//}$ and $10^2-10^5\Omega$.cm for $\rho_{\perp}$ [1,14]

*** the concentration of metal ions in solution during film formation was on the order of $2x10^{-3}$M

interference microscope) the thickness of a thick multiple film obtained by repeatedly using the transferring technique (as described in Chapter 3).

4.4.1 Blank films

The resistivity in the direction perpendicular to the layers (Table 1) for blank films obtained with the methods described earlier (Sections 2.5.1 and 3.5.4) is about $\rho_{\perp} = 10^6$ Ω.cm while the resistivity in the direction parallel to the basal planes is around $\rho_{//} = 10^4 \Omega$.cm, and the ratio $\rho_{\perp} / \rho_{//} = 100$. This is consistent with Divigalpitiya's results [19].

The quasi two dimensional MoS_2 single crystal has a significant electrical anisotropy (see Table 1) resulting from the layered structure. The resistivity across the layers (c-direction) (10^5 Ω.cm [4]) is much higher than that along the layers(10^3 Ω.cm [4]). Of course, as mentioned in Chapter 1 the results reported by different workers significantly differ from one another with the ratio $\rho_{\perp} / \rho_{//}$ varying from 10 to 1000. The higher resistivity perpendicular to the layers presumably arises because potential energy barriers exist between the layers and the current carriers must hop over these barriers (van der Waals gaps). Because there is negligible wave function overlap of the d orbitals between layers, they cannot move in accordance with a band mechanism like they do in the direction perpendicular to c-axis. For a

single crystal, a conductivity difference by a factor of 10^3 or a bit higher in these two characteristic directions has been reported [1,4,14].

The resistivities (Table 1) obtained for the polycrystalline films are higher than those reported for single crystals in both directions. However, it must be recalled that the films we are studying are polycrystalline, hence the electrical properties presented for current parallel to the layers are mainly a reflection of the boundary behavior and can be reasonably expected to show higher resistivity than single crystal.

Comparison of $\rho_{\perp}$ between single crystals and our films is difficult, because single crystal data gives results varying from 10^3 Ω.cm to 10^5 Ω.cm. If we accept the lowest value, we must explain why our value is much higher, because with electrons directly hopping over the van der Waals gaps (a model to be proposed and supported later), our films should have the same $\rho_{\perp}$ value as single crystal.

Poor inter-particle interaction between the platelets in the polycrystalline films may be responsible for the high resistivity perpendicular to the film compared to the single crystal. It was found that the film can be compressed significantly along the substrate when fresh (before drying).

This, of course, results in a shorter film but it was observed that the thickness of this film is only roughly doubled after the compression. However, the compressed film after drying shows a conductivity in the direction parallel to the layers up to two orders of magnitude higher than that of uncompressed one [35]. This, and the smaller density (than that of a single crystal) shown in Tables 2-4, apparently indicate that there exists "free space" within the films, i.e., the platelets are not closely packed in planes parallel to the layers. We think this is a very important observation which could explain the high resistivities (compared to the single crystal results) in both directions, parallel and perpendicular to the layer basal planes. The voids (free space as labelled above) increase the difficulty for current carriers to hop through the film (and result in higher $\rho_{\perp}$). These voids will make the effective conduction section area smaller than that actually used (film thickness multiplied by film width) to calculate the $\rho_{//}$ (then result in higher apparent $\rho_{//}$), although this latter effect will only be the order of a factor of 2.

As we mentioned earlier, rapid heating or cooling of the sample films may create defects within them and we indeed experienced that when this happens the resistivities in both characteristic directions are extremely high (not measurable with our setups). This phenomenon may partially explain the

high resistivities we obtained when we baked the films at 220°C - 250°C with a slow temperature variation, which we thought would be safe. The detailed behavior of these boundaries and defects certainly demands more careful investigations which must, presumably, be fairly sophisticated.

One interesting question that arises is the route of the current carriers in the $\rho_{\perp}$ measurement. When a voltage is applied in the direction perpendicular to the platelets, will the current carriers (a) take straight paths through the layers or will (b) they take zigzag paths only or will (c) they mainly jump at edge sites along the platelet boundaries? We will be interpreting our various results below as evidence for (a).

With a single crystal using the guard ring method, the answer to this question should be straightforward: the carriers jump through the sample along the c-axis. This is a picture taken for granted by all workers working on MoS_2 single crystals. If such a path leads to a relatively low resistivity $\rho_{\perp}$ (10^3 - 10^5 Ω.cm as in Table 1) for the single crystal, the path, and the low resistivity should be observed for our films if model (a) is correct. However, our films show a value of $\rho_{\perp}$ ten times higher than the highest of single crystal results reported. Nevertheless, the effectiveness of

the guard ring in eliminating the current "leakage" out of the cylinder (assuming the central contact is a circular disk) defined by the central contact seems questionable even for single crystals. This means the actual conducting section area may be larger than the area of the contact which has been used to calculate the resistivity $\rho_{\perp}$, and this may leads to a lower apparent resistivity in the c-axis direction for the single crystal. As argued in the appendix, this problem does not seriously affect the calculation of $\rho_{\perp}$ for our very thin films, but it may be significant for thick specimens such as single crystals of several millimeters thick.

Another possible problem with the single crystal is the possibility of special lattice defects that arise during the cleavage of the crystal using cellotape. Such defects, not to be expected on our films, could short-circuit the $\rho_{\perp}$ for a single crystal.

4.4.2 Additive containing films

Table 1 (Page 63) shows how the resistivities are affected by metal ions introduced as in Section 3.3.

The presence of those metal ions at the MoS_2 platelet edges causes a strong increase of the conductivity parallel to the basal plane. The data (Table 1) for all these ions studied, Co^{++}, Ni^{++}, Cu^{++} shows that with ratio as low as 1:100

(guest metal : Mo atoms as the host) we can increase the conductivity by about one order of magnitude.The results shown in Table 1 were obtained from samples with higher composition ratios as shown in Tables 2-4.

The metal ions are thought (Section 3.3.2) to be attached around the platelets at the edge sites. The argument is as follows. There is no reason to discriminate between the OH^- groups on basal planes and the edges in providing adsorption sites for the metal ions. But the "shaking" which causes the OH^- groups on the basal planes to be replaced by organic molecules eliminates these basal adsorption sites.

To prepare inclusion compounds, (where, it will be recalled, shifts in inter-layer spacing are observed) high concentrations of metal ion solutions are used to cause the flocculation of MoS_2 layers. Organic molecules are not involved in doing this. When there exist large number of metal ions such as Ni^{++}, the process

$$Ni^{++} + OH^- \rightarrow (NiOH)^+ \qquad (1)$$

is favored and the combination between these $(NiOH)^+$ and the OH^- (mainly on basal planes)

Table 2 **EG&G ORTEC**

ZAP MICROANALYSIS REPORT

V02.12 15-JAN-91 09:49

ID: JAN15

ELEMENT		WEIGHT PERCENT	ATOMIC PERCENT	INTENSITY (CPS)
S	KA	37.74	64.12	107.35
Cu	KA	1.83	1.57	2.07
Mo	KA	60.43	34.31	2.45

ACCELERATING VOLTAGE:	25.0 KV
SPECIMEN TILT X-AXIS:	30.0 DEGREES
Y-AXIS:	0.0 DEGREES
INCIDENCE ANGLE :	62.38 DEGREES
TAKEOFF ANGLE :	31.55 DEGREES
SAMPLE DENSITY :	4.10 G/CC

*****WARNING*****

ABSORPTION CORRECTION FOR

THE FOLLOWING ELEMENTS IS

LESS THAN 0.7!

S KA = 0.6329

****SPATIAL RESOLUTION OF ANALYSIS****

2.02 TO 6.82 MICRONS

Table 3 **EG&G ORTEC**

ZAP MICROANALYSIS REPORT

V02.12 15-JAN-91 09:49

ID: JAN18

ELEMENT		WEIGHT PERCENT	ATOMIC PERCENT	INTENSITY (CPS)
S	KA	44.24	70.21	222.77
Ni	KA	0.64	0.55	1.47
Mo	KA	55.13	29.24	3.83

ACCELERATING VOLTAGE: 25.0 KV

SPECIMEN TILT X-AXIS: 30.0 DEGREES

Y-AXIS: 0.0 DEGREES

INCIDENCE ANGLE : 62.38 DEGREES

TAKEOFF ANGLE : 31.55 DEGREES

SAMPLE DENSITY : 4.10 G/CC

*****WARNING*****

ABSORPTION CORRECTION FOR

THE FOLLOWING ELEMENTS IS

LESS THAN 0.7!

S KA = 0.6329

****SPATIAL RESOLUTION OF ANALYSIS****

2.02 TO 6.82 MICRONS

Table 4 **EG&G ORTEC**

ZAP MICROANALYSIS REPORT

V02.12 15-JAN-91 09:49

ID: JAN18 60X

ELEMENT		WEIGHT PERCENT	ATOMIC PERCENT	INTENSITY (CPS)
S	KA	43.6	69.82	223.51
Co	KA	0.59	0.46	0.47
Mo	KA	55.81	29.72	3.91

ACCELERATING VOLTAGE: 25.0 KV

SPECIMEN TILT X-AXIS: 30.0 DEGREES

Y-AXIS: 0.0 DEGREES

INCIDENCE ANGLE : 62.38 DEGREES

TAKEOFF ANGLE : 31.55 DEGREES

SAMPLE DENSITY : 4.10 G/CC

*****WARNING*****

ABSORPTION CORRECTION FOR

THE FOLLOWING ELEMENTS IS

LESS THAN 0.7!

S KA = 0.6329

****SPATIAL RESOLUTION OF ANALYSIS****

2.02 TO 6.82 MICRONS

$$(NiOH)^{+} + OH^{-} \rightarrow Ni(OH)_2\downarrow \qquad (2)$$

causes the collapse of double layer repulsion which in turn leads to the flocculation of the suspension.

However, during our film preparation, as described in the standard procedure, the water immiscible organic molecules replace the OH^- groups on the basal planes because the bonding between these OH^-s and the basal sites is weak. The basal planes thus no longer attract the metal ions, and the edge sites are the only places still covered by OH^- ions (because of stronger bondings). If the metal ions somehow existed on the basal planes in appreciable amounts, we should be able to detect this simply by XRD. The XRD patterns of additive included films show no shift of the {001} line from its position with a blank film (additive free), indicating no adsorption of metal ions on the basal planes in our films.

Fig.16-18 show variation of $\rho_{//}$ of additive containing films as a function of the concentration of the metal ions used (Ni^{++}, Co^{++} and Cu^{++}). Films can be made within certain range of concentration (not so high as to cause flocculation but high enough to show a detectable effect). Higher metal ion concentration (the pH of the MoS_2 suspension is 7 before the addition of the ionic solutions) results in a higher

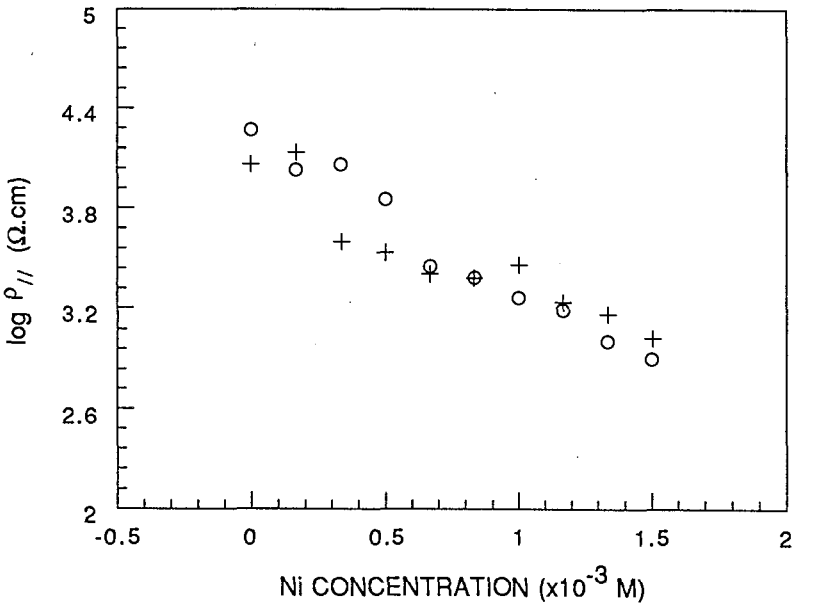

Fig.16 $\log\rho_{//}$ vs concentration of additive {$Ni(NO_3)_2$ or $NiCl_2$}

\+ where additive = $Ni(NO_3)_2$

o where additive = $NiCl_2$

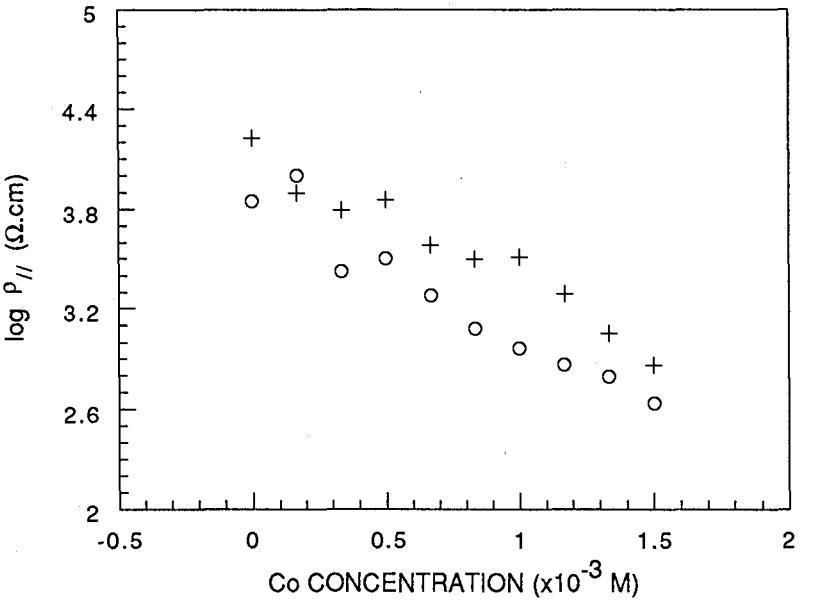

Fig.17 $\log\rho_{//}$ vs concentration of additive {$Co(NO_3)_2$ or $CoCl_2$}

\+ where additive = $Co(NO_3)_2$

o where additive = $CoCl_2$

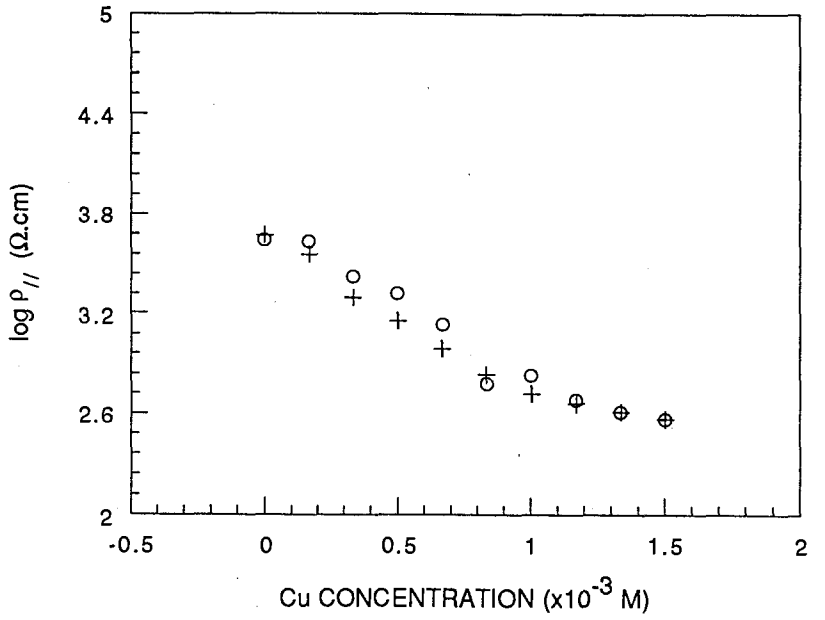

Fig.18 $\log\rho_{//}$ vs concentration of additive {$Cu(NO_3)_2$ or $CuCl_2$}

\+ where additive = $Cu(NO_3)_2$

o where additive = $CuCl_2$

conductivity of the additive containing films in the direction parallel to the platelets. This is easily understood qualitatively. With higher ion concentration, we have more metal ions at the platelet edge sites injecting carriers. Too high an ion concentration causes flocculation as discussed earlier. The resistivity $\rho_{//}$ seems to vary approximately exponentially with the concentration of ions in the solutions from which the films are prepared. The reason for the apparent exponential variation is not clear.

The data for additive containing films in Table 1 were collected from the measurements on samples with maximum metal involvement, say, $2x10^{-3}M$ (at this concentration, flocculation was observed to start occurring) or even higher (usually even when partial flocculation occurs we are still able to obtain a film reasonably long for the resistivity measurement).

The platelet lateral size is estimated to be less than a few hundred angstroms across based on the ratio between the number of adsorbed metal and Mo atoms in the additive included films. The length of the sample whose resistivity was under study is about 0.5mm laterally, which means there are many boundaries in the area of interest (between Ag strips B and C in Fig.11). This is in favor with the statement that boundary behavior dominates. We attempted to determine the maximum MoS_2 platelet size by the amount of

bridging metal ions adsorbed on the edge sites of these layers (see below). One problem arising here is that we can not easily determine what fraction of the available edge sites are occupied by the bridging ions. Obviously, the ratio between adsorbed metal ions and Mo atoms significantly depends on the lateral size of platelets. However if we assume that the edge sites are completely covered by metal ions (due to reactions 1 and 2) at a concentration just before rapid flocculation of the particles, we can obtain the platelet size from the metal/Mo ratio. If the coverage is less than 100%, then the size must be less than the calculated value.

To estimate the average size of the platelets, a couple of assumptions are made.

(1) each platelet is a square sheet, with each side to be d Å.

(2) every edge site is occupied by one and only one included metal ion.

The thickness of one single layer is t = 3.19Å and the density of 2H-MoS_2 is ρ = 4.92g/cc, i.e. $\rho = 4.92 \times 10^{-24}$ g/Å^3 while the molar mass of is M = 160g.

Then the ratio of $\frac{Ne}{Nb} = \frac{4}{(\frac{d^2 \rho t 6.02 \times 10^{23}}{M})^{1/2} - 4}$

where N_e and N_b are the numbers of edge sites and basal sites on one single layer respectively. With the assumptions made above, $\frac{N_e}{N_b} \approx \frac{N_M}{N_{Mo}}$ where N_M and N_{Mo} are the number of additive metal ions and the number of Mo atoms in the sample film respectively. From Tables 2-4, we have $\frac{N_M}{N_{Mo}}$ = 1.57:34.31; 0.55:29.24; 0.46:29.72 for Cu, Ni, Co included films respectively which in turn yield d = 360Å, 875Å, 1063Å as the maximum average platelet diameter. These values compare favorably with the size of single layers or restacked platelets (about 1000Å) estimated by transition electron microscopy (TEM) (private communication).

The observed resistivity perpendicular to the basal planes (Table 1) provides an independent argument that the metal ions are primarily at edge sites. This argument is made based on the fact that the presence of foreign metal species did not improve or even change the resistivity $\rho_\perp$. From early studies [4], the metal ions seem to inject carriers at all points, so basal metal ions (if any) could be expected to increase the conductivity normal to the basal planes.

The suggestion that electrons are activated over the van der Waals gap is supported by the $\rho_\perp$ measurements of Table 1. The fact that $\rho_\perp$ is unchanged (from the metal ion free film) provides such evidence. Although the voltage used to measure $\rho_\perp$ is low (several mV), a strong electrical field ($\sim 10^5$V/m)

along the direction perpendicular to the layers is established inside the very thin film. This very strong electrical field not only eliminates the contact resistance problem [4] but also favors the direct jumping model for it is reasonable to infer that this strong electrical field in the direction normal to the layers within the film will overwhelmingly drive the carriers through the film in the direction of the field $\mathbf{E}_c$. In addition, if zigzag paths were taken by the carriers, the metal ions at the edge sites should have an effect on the $\rho_\perp$ similar to that for $\rho_{//}$.

The diagram shown in Fig.19 should help one understand the mechanism proposed by the author qualitatively. In a $\rho_\perp$ measurement, carriers (say, the electrons) are injected into the sample from atop the film. Instead of going towards theboundaries by taking advantage of the low $\rho_{//}$ paths in the basal planes and then jumping at the edges (zigzag paths), most of them more likely jump over the van der Waals gaps from the points of injection to the neighboring layer underneath because as we mentioned the electrical field $\mathbf{E}_c$ is very strong and $\rho_{//}$ is also high even though lower than $\rho_\perp$. There should also be a potential barrier between a edge site and a basal site though it could be lower than that between two basal sites. This is thought to explain why the existence of metal ions at the edges does not help improve the $\sigma_\perp$, at least much less significantly than it does to $\sigma_{//}$.

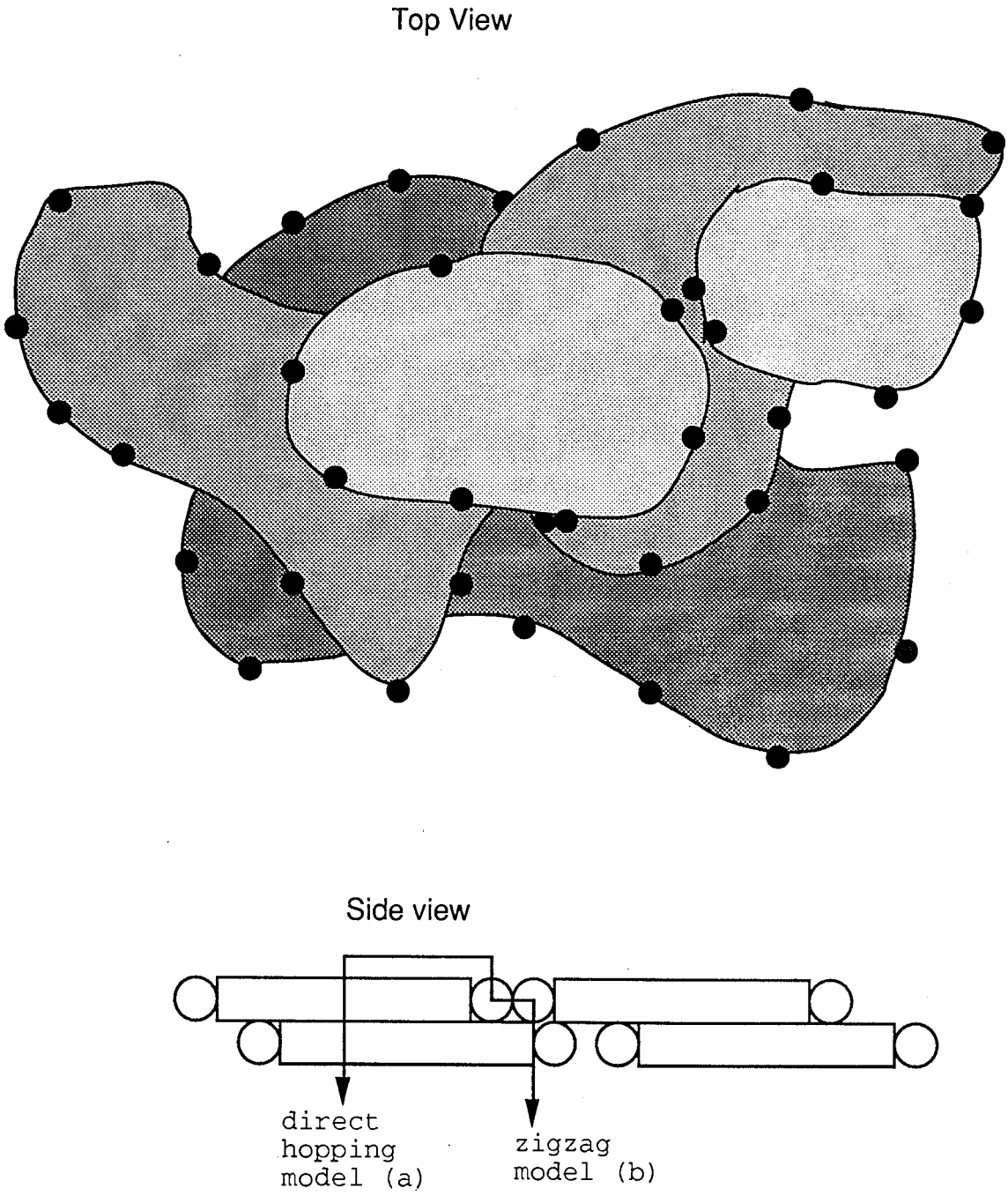

Fig.19 Schematic picture of the film

Parallel to the basal planes the resistivity is lowered by metal ions. With no metal ions, the electrons have to jump at the boundaries which results in significantly higher resistivity compared with that in a single crystal. The metal ions at these boundaries undoubtedly serve as short-circuit paths for the carriers and thereby account qualitatively for the reduction in resistivity in the direction parallel to basal planes by one order of magnitude. The metal ions could act as "bridges" with the carriers moving from the platelet to the metal ions and then to the neighboring platelet, or it could simply be the excess carriers at the boundary (Fig.13-14) that cause shorting between the boundaries.

4.4.3 Activation energies

Like resistivities, the reported values of the activation energies of single crystal are scattered, from 0.14eV to 0.87eV [1]. In Fig.20 - Fig.23, we show Arrhenius plots of the resistivity vs temperature for blank and additive containing MoS_2 films. From the temperature dependence experiments, several activation energies are obtained as:

	blank film	Ni^{++} included film
$\varepsilon^{//}_a$	0.29 eV	0.22 eV
$\varepsilon^{\perp}_a$	0.18 eV	0.18 eV

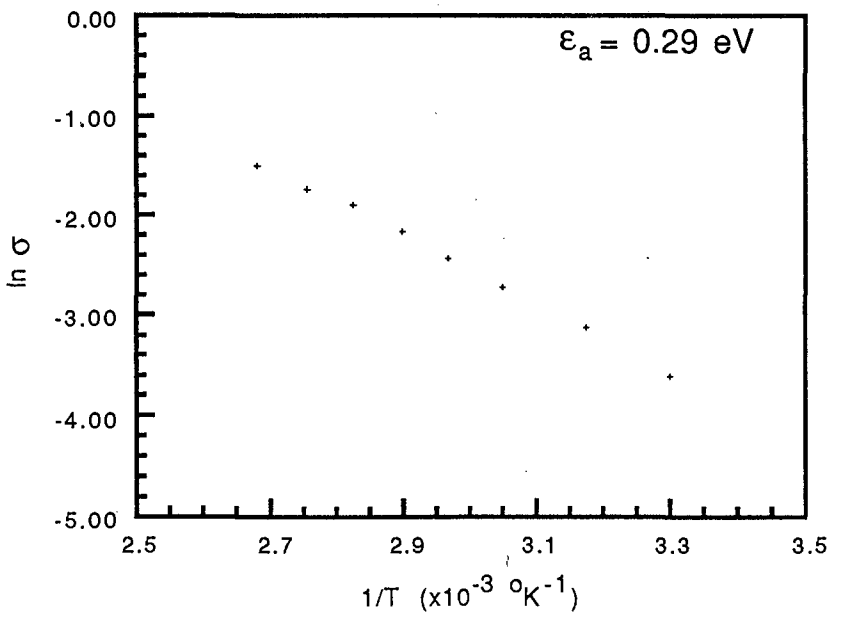

Fig.20 Temperature dependence of $\sigma_{//}$ for a blank film. measurement made with a four-point-probe circuit. The number at the upper right corner is the slope (hence the activation energy) of a straight line that best fits the points in the figure. There is a offset (not indicated) on the Y axis ($\ln\sigma$), which does not affect the slope (activation energy)

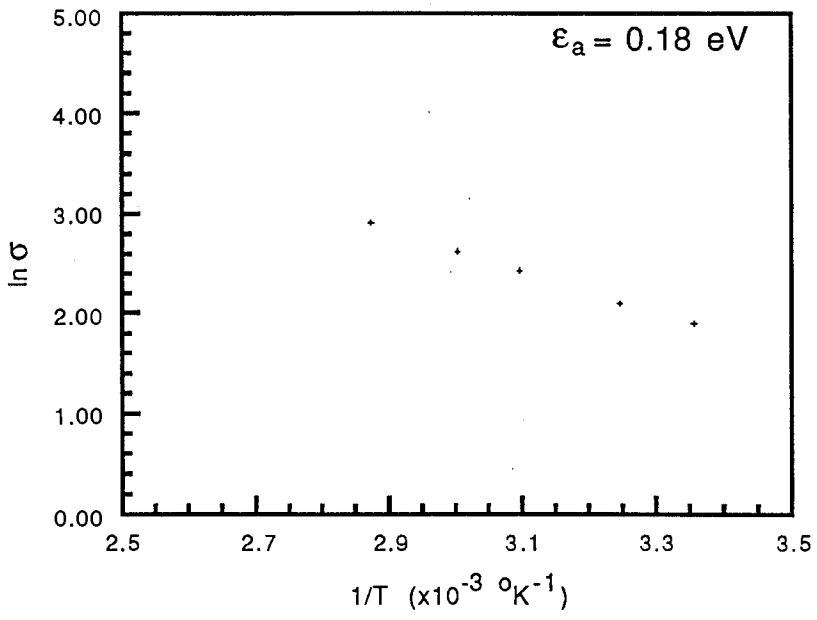

Fig.21 Temperature dependence of $\sigma_{\perp}$ for a blank film. measurement made with a guard ring circuit. The number at the upper right corner is the slope (hence the activation energy) of a straight line that best fits the points in the figure. There is a offset (not indicated) on the Y axis (lnσ), which does not affect the slope (activation energy)

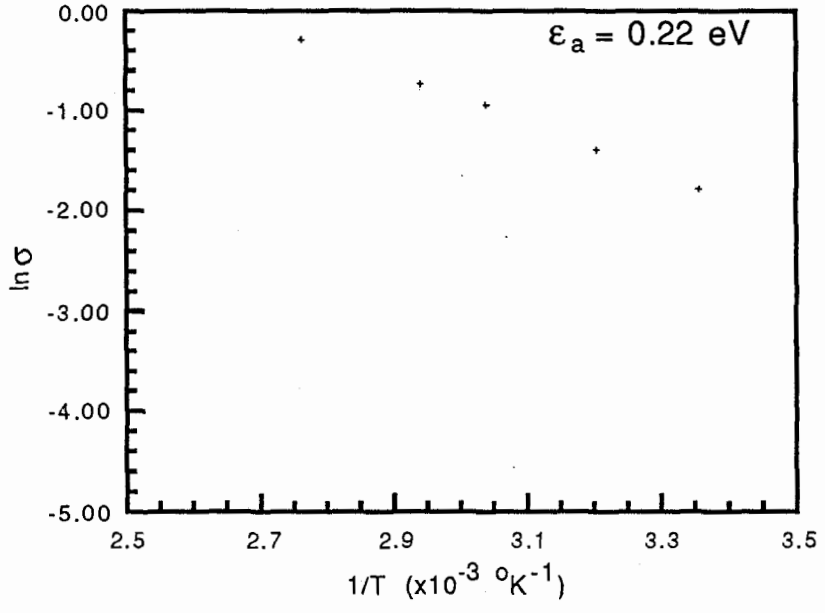

Fig.22 Temperature dependence of $\sigma_{//}$ for a Ni bridging film. measurement made with a four-point-probe circuit. The number at the upper right corner is the slope (hence the activation energy) of a straight line that best fits the points in the figure. There is a offset (not indicated) on the Y axis (lnσ), which does not affect the slope (activation energy)

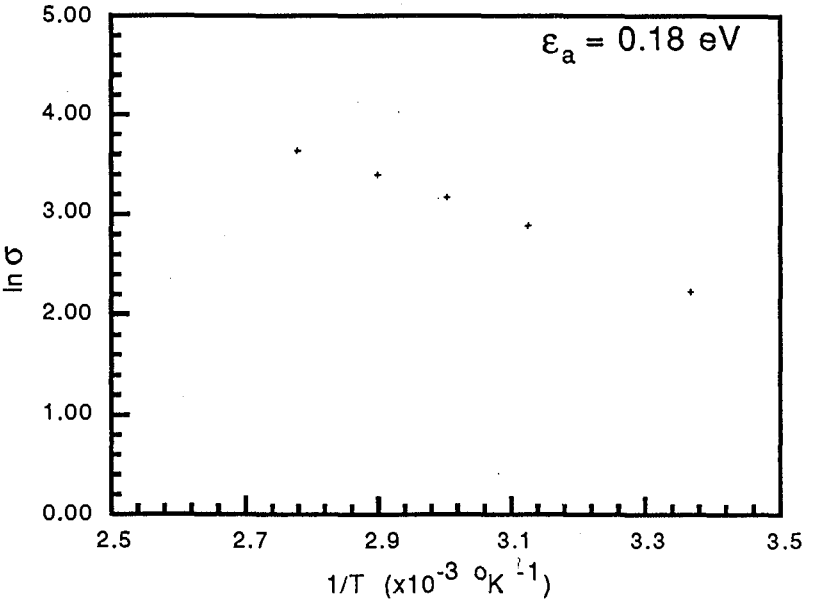

Fig.23 Temperature dependence of $\sigma_{\perp}$ for a Ni bridging film. measurement made with a guard ring circuit. The number at the upper right corner is the slope (hence the activation energy) of a straight line that best fits the points in the figure. There is a offset (not indicated) on the Y axis (lnσ), which does not affect the slope (activation energy)

where $\varepsilon^{//}_a$ is the activation energy in the direction parallel to basal planes and $\varepsilon^{\perp}_a$ is the activation energy in the direction perpendicular.

From the above data, we can infer that the metal additives at the edge sites are very active in the parallel direction. For the Ni^{++} included film, the $\varepsilon^{//}_a$ is reduced by 32% and this parallels the reduction of $\rho_{//}$. These $\varepsilon^{//}_a$ values can be compared to those for single crystals [1] and such a comparison may parallel that between $\rho_{//}$s of a single crystal and our polycrystalline films. Both comparisons favor the "boundary domination" statement.

The apparent difference between $\varepsilon^{//}_a$ and $\varepsilon^{\perp}_a$ as well as the similar $\varepsilon^{\perp}_a$ for both additive containing and additive free films also indicates the direct jumping model, otherwise, if zigzag paths were taken, we should have obtained similar values for $\varepsilon^{//}_a$ and $\varepsilon^{\perp}_a$ and also the metals at the boundaries should have effected $\varepsilon^{\perp}_a$ for the Ni included film. We can use the same argument in terms of band models presented in Section 4.3 to explain the influences of the added metals on the activation energies.

The observation that $\varepsilon^{\perp}_a$ is 0.18eV and is different (lower) from $\varepsilon^{//}_a$ for the blank film suggests that this is the activation energy for crossing the van der Waals gap. The

observation that the value is independent of the Ni^{++} additive provides further evidence that there are no ions on the basal planes for if there were ions there one would expect them to influence the activation energy $\varepsilon^{\perp}_{a}$.

4.4.4 Polymer sandwiches

As we mentioned earlier (Section 3.5) styrene included films always consist of two phases, and it is a reasonable inference that the properties of these films will depend on the ratio of these two phases. As stated in Section 3.5, one phase corresponds to additive-free MoS_2, the other is attributed to sandwiches with a monolayer of polystyrene between adjacent MoS_2 layers. We may be able to get some qualitative feeling on the fractions of these two phases from the ratio of intensities of the two peaks in XRD (Fig.5) but it still remains hard to correlate this ratio to the electrical behavior of such a film quantitatively. Another difficulty in comparing styrene included MoS_2 films to inorganic MoS_2 films is that the organic sandwiches have actually gone through a different procedure, hence one can not make quantitative comparisons between these organic sandwiches and inorganic films treated differently. Finally, organic sandwiches are likely to be destroyed by even moderate heating though one may find polystyrene quite stable at room temperature.

One should understand that a one molecular thick "polystyrene" sheet is expected to be different from bulk polystyrene in such respects as their melting points and decomposition temperatures.

The concept of polymerization of a one-molecular thick styrene sheet demands some clarification. The polymerization of a one-molecule thick styrene sheet in our case means, on one hand, these styrene monomers trapped between MoS_2 platelets may link to each other to form a polystyrene sheet; on the other hand, some styrene monomers may simply attach themselves to the basal planes of the platelets confining them. Either way, the styrene molecules will be more stable against evaporation. The increased stability evidences itself by showing a stable {001,phase 1} peak (after the polymerization) that characterizes the polystyrene sandwich.

Table 5 shows the electrical resistivity data for polymer included MoS_2 spread films. One may notice that the data presented for organic sandwiches show some overall difference from that for organic-free films. For instance, the parallel resistivity $\rho_{//}$ is five times lower than that of previously studied blank films. This was thought to be caused by the remainder of water molecules in the films, existing because we could not heat the sandwiches at 220°C, temperature at which the adsorbed water molecules are believed to detach

Table.5 Resistivities of polymer-including films

	$\rho_{//}$ (Ω.cm)	$\rho_{\perp}$ (Ω.cm)
additive free film	$2x10^3$	$7x10^8$
Ni^{++} containing	$5x10^2$	$7x10^8$
Co^{++} containing	$8x10^2$	$6x10^8$
Cu^{++} containing	$7x10^2$	$7x10^8$

from the platelets [19]. However, distilled water itself has a fairly high resistivity, so it is hard to be convinced that this higher conductivity is caused by the water alone. We think that this low resistivity is probably because of the existence of some undesired ions that are electrically active in water. Residual Li is a strong possibility. More importantly, it is also possible that due to the lack of high temperature dehydration, the transition from octahedral to trigonal prismatic coordination (2H) is incomplete and the octahedral MoS_2, which is thought to be semi-metallic [1], will increase the conductivity $\sigma_{//}$ of a pure 2H-MoS_2 film.

Polystyrene is a very good insulating material. When this insulator is inserted in between the semiconducting MoS_2 layers, it should make it much more difficult for the carriers to hop from one layer to the other and therefore make the $\rho_{\perp}$ very high. As shown in Table.5, the resistivity of film with polystyrene involved separating MoS_2 layers from each other has a high value of $\rho_{\perp}$ about 10^9 Ω.cm. On the other hand from the comparison of $\rho_{//}$ in Table 1 to $\rho_{//}$ in Table 5, the polymer apparently only affects the resistivity by a factor of 5 or so in the direction parallel to the basal planes (which was explained above). The reason that the polymer does not more strongly affect the resistivity parallel to the layers is presumably because that the current carriers injected onto the MoS_2 layers will move along the

layers until they reach the boundaries. The polymer trapped between the layers does not affect the motion of the carriers along the basal planes. It does, however, drastically increase the difficulty to go through the sandwiches. As a result we observe the highly increased $\rho_{\perp}$ and somewhat stable $\rho_{//}$ for the polymer sandwiches. These facts also indicate that the polymer is not significantly adsorbed at the edges, which is consistent with the model discussed elsewhere [19,32]. Up to now, we have achieved an electrical anisotropy characterized by a resistivity ratio of about 10^6.

4.4.5 Doubly modified films

The two modifications described above, the metal ion addition and the styrene addition, were of basic interest in identifying the conduction mechanism in our composite films. For practical reasons, it was hoped to combine the two positive (desirable) effects, the increased parallel conductivity $\sigma_{//}$ with bridges and the reduced perpendicular conductivity $\sigma_{\perp}$ with the polymer, to achieve even higher anisotropy. However, the data, as shown in Table.5 indicates that, with the presence of polymer, the metal bridging effect is masked (at least partially). This is understood as that the polymer not only separates the layers but also partially blocks the bridges, leaving the bridges less effective or even non-operational. Unfortunately, from the information collected, it is not possible to make a quantitative analysis

as to the contribution from the bridges and the insulating layers. The model used to account for the observed results is therefore qualitative.

4.5 PROJECTED APPLICATIONS

The versatility of the techniques used for this study and the well constructed films may have practical as well as basic significance.

4.5.1 The techniques

The technique used here to exfoliate layered MoS_2 can be and has been used to treat other materials with similar structure [36]. And also, this technique can be employed with benefit in the study of catalysis [30]. As described earlier, this is in fact a very convenient way to make inclusion compounds hosted by the exfoliated material, a form of composite. The technique to form the highly oriented films is analogous to the Langmuir-Blodgett (LB) technique [37] which however only treats organic molecules with both polar and non-polar ends. The exfoliation and film fabrication techniques enable one to make molecular sandwiches and freely control the architecture. The technique itself is very easy to apply and very economic. Unlike the LB technique, it does not require expensive equipment.

We actually used this technique to make insulating Al_2O_3 thin films with limited success. It was also proposed to make Al_2O_3/MoS_2 alternating films, but substantial difficulties may be expected because of the substantial difference between the thicknesses of these two kinds of platelets (Al_2O_3 platelets are about 50Å thick while MoS_2 platelets only several angstroms thick) though this might be a useful composite for Al_2O_3, like polystyrene, is an excellent insulator.

4.5.2 The films

Using the MoS_2 layers as the skeleton, one can construct different kinds of films with a variety of physical properties, for instance, with a high electrical anisotropy as shown in this thesis work. The inclusion of a wide range of guest species, which is made possible by using the techniques we developed and described in this thesis, can also enhance the magnetic properties of the original materials [39 - 41]. Furthermore, microwave applications, using the films as X-ray mirror, etc. all seem more feasible as the research proceeds further.

4.6 EXPECTED EXTENSIONS OF THIS PROJECT

This project explored the probability of modifying exfoliated MoS_2 single molecular layers, based on the different chemical nature of the sites on them. Further work along this line should be rewarding.

One suggestion would be to combine this work with the well developed LB techniques [42] which solely employ amphiphilic organic molecules as construction materials. By using both techniques, sandwiches of different contents could be easily made just by alternating the molecular layers (LB or composite films) at specific positions as desired.

The introduction of foreign species in the way discussed in this thesis can change the carrier type of the original material. Hence, it can be hoped that the carrier density in the films can be freely controlled by controlling the addition of guest elements. The distortion of the 2H-MoS_2 energy band structure due to the inclusion of foreign species can be quantitatively studied and should yield valuable information on such an artificial molecular assembly. As we now understand it, the properties of the grain boundaries (or edge sites) dominate the film properties and the band mechanism in an additive included film is a clue to further study, the detailed boundary behavior which is believed to be significantly different from that of the bulk region.

Using additive included MoS_2 films as microelectrodes for an intercalation battery may be interesting and could be productive in improving the battery efficiency and providing

a good alternative way to adjust the terminal voltage of such batteries.

The reverse process of this work, i.e., to increase the conductivity $\sigma_{\perp}$ and reduce the conductivity $\sigma_{//}$ seems possible. This could be done by attaching species which could enhance the originally existing energy barriers at the boundaries,to the MoS_2 layer edges. Instead of separating the layers with insulating materials like polystyrene, we may choose materials such as a conducting polymer which could bridge the electricity carriers through the van der Waals gaps. In fact, we did try to include pyrrole (polypyrrole is conducting) in the film but it was unsuccessful maybe due to the slight solubility of pyrrole in water and our procedure seems to require perfectly water immiscible organic solvents to make the spread films.

Another possible application that could be explored is the possibility of using these kinds of films as membrane filters.

4.7 RECOMMENDATIONS FOR FUTURE STUDY

By now, there has been a large number of techniques developed to form new materials possessing different kinds of interesting and unique properties. New ones keep emerging constantly. As described in this thesis, the technique

developed in our laboratory and used for this thesis project has its uniqueness and advantages in dealing with the particular semiconductor compound MoS_2 and other layered compounds as well. The high electrical anisotropy achieved in this project is only a primary attempt toward making new materials with new structures which in turn result in specific physical properties as desired. The main idea guiding this research is to modify the quasi-two dimensional MoS_2 layers by attaching proper foreign species to certain sites. The film formation technique employed here only requires the organic solvent used to be water immiscible and this allows a great number of organic solvents to be usable.

The electrical properties of MoS_2 films as well as their variations have been the primary concern of this project but other aspects should be equally valuable. For instance, the magnetic properties of intercalates with exfoliated MoS_2 layers as host have been under study by another group in this department and they have observed interesting phase transition phenomenon [43].

Using the exfoliation and film fabricating techniques described above, we can expect more materials with interesting properties to be made. As an example, we all know that MoS_2 has long been used as a lubricant because of the easy relative sliding between layers. Now, with our

techniques, we should be able to optimize the quality of this lubricant like we optimize its electrical conductivity.

As coating material, we are now able to coat almost any surface with an extremely thin layer of MoS_2 and of even greater interest, we can modify the properties of such coatings in many ways if desired.

It is inevitable that we can only make polycrystalline MoS_2 films due to the nature of the starting material and the procedures involved. Under a scanning electron microscope, we can see that the MoS_2 layers, after exfoliation, are of different lateral sizes and the variation in layer size is beyond our control at the present stage. The size of the layers seems fairly important for our purposes, because the smaller the layers, the higher the the ratio between the number of edge plane sites and the number of basal plane sites and the more boundaries. As we repeatedly claimed, the properties of the composite films are mainly determined by the properties of the boundaries in them. The control over the layer size should yield significant freedom in controlling the film properties.

The technique used to insert certain organic materials in between the host layers is, of course, not the only one satisfying this purpose, and as mentioned earlier the LB

technique should be a reasonably good alternative. But, while LB technique could offer a large area and uniform organic molecules which do not have to be completely water immiscible (in fact, the LB technique employs amphiphilic molecules), we should expect tremendous difficulty in an attempt to place these organic layers between every MoS_2 layer in an A-B-A-B order, because so far we are unable to produce a MoS_2 film of one molecule thickness.

The transferring technique we used to transfer films from water wettable substrates to non-wettable ones is surely imperfect. Though it was claimed that this technique could retain the quality of the original films, film cracking is almost always observed. Furthermore, more serious damage at a microscopic scale by employing this technique seems possible, so this step should be further optimized.

Similar to the LB technique, we can directly obtain films from the water organic interface by simply inserting the non wettable substrates into the suspension phase and raise it again, but this gives poorer uniformity. This poorer uniformity could be improved one way or another.

CHAPTER V CONCLUSIONS

It has been shown that the flocculation phenomenon is very important for the present work and other exfoliated MoS_2 related interests as well. The flocculation of an MoS_2 suspension is caused by the neutralization of the OH^- groups adsorbed around the MoS_2 single layers. Flocculation had been a negative effect for the purpose of this project though it has positive aspects for other interests.

From the experimental results of resistivities in directions normal and parallel to the layer basal planes, it is concluded that the defects (e.g. boundaries, voids inside the films) dominate the film conducting properties parallel to the layers of the MoS_2 film. Conductivity through (perpendicular to the layers) the film was not noticeably affected by platelet boundaries.

Metal additives have been successfully attached to the edge sites of the MoS_2 layers. According to our model the metal additives around the boundaries of the platelets form conducting loops by injecting current carriers into the host, and as a consequence, the original carrier type of the film (p-type) can be changed or modified.

From the concentration of metal ions in an additive included film, the size of the platelets was estimated to be less than one thousand angstroms in diameter.

The resistivity $\rho_{//}$ of the MoS_2 film along the basal planes is reduced by a factor of 10 when Cu^{++}, Ni^{++} or Co^{++} are adsorbed at the platelet edges. Similarly, the activation energy ε''_a for the resistivity in such additive included films in this direction is also reduced by about 32%, indicating strong influence from ions adsorbed on the platelet edges. On the other hand, these metal additives showed no significant influence over the conductivity $\sigma_\perp$ in the direction normal to the layers.

The lack of an effect of ionic additives on the resistivity normal to the basal planes leads to the conclusion that when an external voltage is applied normal to the film, the current carriers in the film move in accordance with a hopping mechanism across the van der Waals gap as they presumably do in a single crystal. The activation energy to cross the van der Waals gap is 0.18eV. These observations therefore lead to the abandoning of the zigzag path model, which though appeared logical especially with the metal bridging films because these bridges did reduce the potential barriers at the boundaries. The observation also supports further the conclusion that the metal ions are found only at

the circumference of the platelets. Also in contrast with the observation of inter-layer spacing changes with inclusion compounds (with metal ions present on basal planes), we find no such changes in the additive included films. This indicates no metal ions on the basal planes of an additive included film.

A modified procedure to include styrene molecules between the layer basal planes has yielded a greatly enhanced resistivity in the direction perpendicular to the basal planes. The original resistivity of $\rho_{\perp}=10^{6}$ ohm.cm in this direction with a unmodified film was increased by a factor of 10^{3} to $\rho_{\perp}=10^{9}$ ohm.cm.

The combination of styrene inclusion and metal additive modification has resulted in the high electrical anisotropy by a factor of 10^{6} in the composite films described in this thesis. This is not only a valuable achievement by itself, but also indicates a high potential for applications.

In conclusion, we strongly feel that there is much room for improvement in the way the films are made and more extensive research seems necessary and promising.

APPENDIX Validation of Single Dot Approximation

When two resistors R_0 and R_1 are combined in parallel and the resistance ratio is large, say 1:100, then the effective resistance of such a combination will be approximately R_0.

Let the resistance corresponding to the area of the center contact be denoted as R_0 . When the outer contact, the guard ring, is removed in the $\rho_\perp$ measurement with a guard ring, the longitudinal current leakage should in principle be taken into consideration when calculating the resistance. With our samples, the resistivity in the plane (longitudinal dimension) is about $\rho_{//}=10^4$ ohm.cm and the $\rho_\perp$ is 2 orders higher in magnitude, i.e. 10^6 ohm.cm. The radius **r** of the metal dot evaporated is 1 mm, and the typical film thickness is t=300 Å. With guard ring method, the resistance $R_\square$ across a film is typically a few hundred ohms. Now, we wish to demonstrate that the current leakage due to the removal of the guard ring is negligible for these particular samples.

When longitudinal current leaks radially through an excess area defined by a radius **r+x** (refer to Fig.24, P.105), the extra resistance, which would be considered to be in parallel with R_0 , can be estimated as

$$R_1 = \rho_{//} \frac{x}{2\pi rt}$$

To make $R_1 = 100R_0$ (sufficient for the accuracy at which we discuss our experimental results), say 10^4 Ω

$$x = \frac{2\pi rt \cdot R_1}{\rho_{//}} = \frac{2 \cdot 3.14 \cdot 0.1 \cdot 300 \cdot 10^{-8} \cdot 10^4}{10^4} = 1.884 \times 10^{-5} \text{ cm.}$$

This makes $\frac{x}{r} = 1.884 \times 10^{-4} = 0.01884\%$.

The resistance R' of the leaking ring (inner radius r and outer radius r+x) in the direction normal to the layers can be denoted as

$$R' = \rho_{\perp} \frac{t}{\pi(r+x)^2 - \pi r^2} >> R_0$$

Hence we can regard R_0, R_1, R' as to be in parallel (roughly), and R_0 is the smallest one, as is shown, much smaller than R_1 and R'. Therefore, the measured resistance by single dot method

$$R_{eff} \cong R_0$$

which means the single dot approximation is reasonably accurate and the guard ring is not needed for our thin film samples. A parallel argument to the above can be made with data for organic sandwiches and a similar conclusion can be drawn.

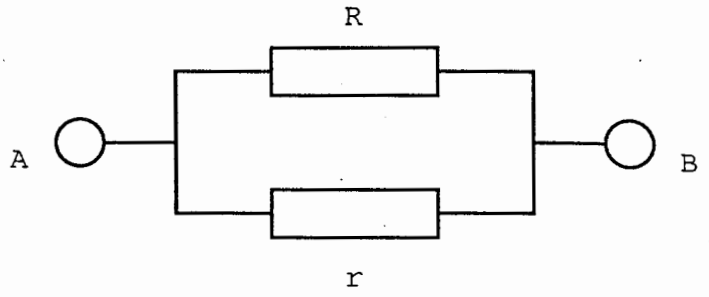

well known fact: when R >> r, then

$R_{AB} \approx r$

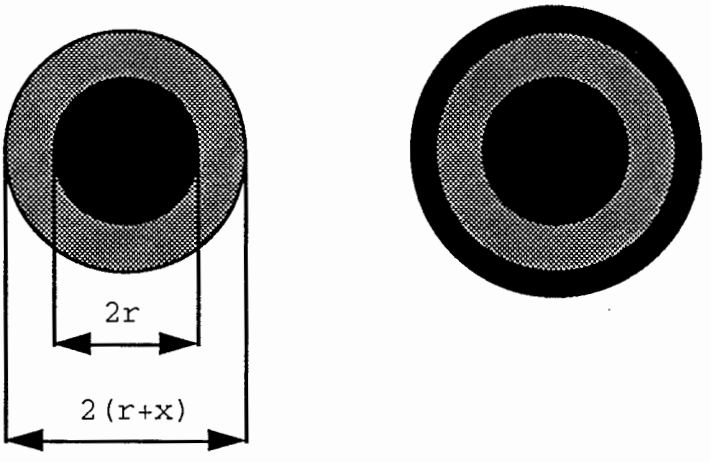

Single dot approximation Guard ring

meatl covering area

uncovered film

Fig.24 Single dot approximation

REFERENCES

1. J.A.Wilson and A.D.Yoffe, 1969, Adv. Phys. 18,193

2. L.H.Brixner and G.Teufer, 1963, Inorg. Chem. 2,992

3. G.D.Guseinov and A.I.Rasulov, 1966, Phys. Stat. Sol. 18,911

4. A.H.Thompson, et. al., 1972, Physical Review B, 5, 2811,

5. S. Graeser, 1964, "Schweiz Min Pet Mitt", 44, 121

6. D.E.Gray, 1972, Am. Inst. Phys. Handbook, 3rd ed.

7. Y. Takeuchi and W. Nowacki, 1964, Schweiz. Min. Petr. Mitt, 44, 105

8. L. F. Mattheiss, 1973, Phys. Rev. B8, 3719

9. B.L.Evans and P.A.Young, 1965, Proc. R. Soc. A, 284, 402

10. R. Mansfield and S.A.Salaam, 1953, Proc. Phys. Soc. B 66, 377

11. R. Fivaz, 1967, J. Phys. Chem. Solids, 28, 839

12. T. Wieting, 1968, Ph.D. thesis, Cambridge

13. R. F. Shaw, 1969, Ph.D. thesis, Cambridge

14. A. Souder and D. E. Brodie, 1971, Can. J. Phys. 49, 2565

15. R. Fivaz and E. Mooser, 1967, Phys. Rev. A 163, 743

16. T. J. Wieting, 1970, J. Phys. Chem. Solids 31, 2148

17. T. J. Wieting and A. D. Yoffe, 1970, Phys. Stat. Solid 37, 353

18. R. D. Audas, 1983, Ph.D. thesis, Simon Fraser

19. W. M. Ranjith Divigalpitiya, R.F. Frindt and S.R.Morrison, 1990, Thin Solid Films, 186, 177

20. S. H. El-Mahalawy and B. L. Evans, 1977, Phys. Stat. Sol. (B), 79, 713

21. B. L. Evans and R. A. Hazelwood, 1971, Phys. Stat. Sol. (A), 4, 181

22. H. Schafer, 1964, Chemical Transport Reaction. AP,NY

23. A. A. Al-Hilli and B. L. Evans, 1972, J. Crystal Growth 15, 93

24. L. E. Scriven and C. V. Sternling, 1960, Nature 187, 186

25. M.B.Dines, 1975, Mat. Res. Bull. vol. 10, pp. 287-292

26. Per Joensen, R. F. Frindt and S. Roy Morrison, 1986, Mat. Res. Bull. 21, 457

27. Bijan K. Miremadi, Timmothy Cowan and S Roy Morrison, 1991, J. Appl. Phys. 69, 6373

28. D. Yang, S. Jimenez, W.M.R.Divigalpitiya, J.C.Irwin and R.F.Frindt, 1991, Physics Review (B) 43, 0

29. Robert B. Somoano and Jhon A. Woollam, 1979, "Intercalated Layered Materials", 307-319

30. Bijan K. Miremadi and S Roy Morrison, 1988, J. Catal. 112, 418

31. Michael A. Gee, R.F. Frindt, P. Joensen and S.R. Morrison , 1986, Mat. Res. Bull. 21, 543

32. W. M. R. Divigalpitiya, R.F. Frindt and S.R. Morrison, 1989, Science,246,369

33. W. M. R. Divigalpitiya, R.F. Frindt and S.R. Morrison, 1991, J. Mater. Res. 6, 1103

34. W. M. R. Divigalpitiya, to be published

35. W. M. R. Divigalpitiya, unpublished results

36. Bijan K. Miremadi and S Roy Morrison, 1990, Mat. Res. Bull., 25, 1139

37. K. B. Blogget, 1935, J. Am. Chem. Soc. 57, 1007

38. "Fundamentals of Chemistry", Frank Brescia, John Arents, Amos Turk, 1966 AP

39. P. Schurer, J. L. LaCombe, T. L. Templeton, A. S. Arrott and R.F.Frindt.
$5M^3I$, Pittsburgh. 1991

40. A. S. Arrott, T. L. Templeton, X. Z. Li, and M. A. Gee
$5M^3I$, Pittsburgh. 1991

41. R. F. Frindt, A. S. Arrott, S. R. Morrison, B. Heinrich, T.L.Templeton, R. Divigalpitiya, M. A. Gee, and P. Joensen.
$5M^3I$, Pittsburgh. 1991

42. H. Tang, Z. Q. Zhu, to be published